DISSERTATIONES
BIOLOGICAE
UNIVERSITATIS
TARTUENSIS
323

RIIN KONT

The acquisition of cellulose chain by a processive cellobiohydrolase

DISSERTATIONES BIOLOGICAE UNIVERSITATIS TARTUENSIS
323

DISSERTATIONES BIOLOGICAE UNIVERSITATIS TARTUENSIS
323

RIIN KONT

The acquisition of cellulose chain by a processive cellobiohydrolase

UNIVERSITY OF TARTU
Press

Chair of General and Microbial Biochemistry, Institute of Molecular and Cell Biology, Faculty of Science and Technology, University of Tartu, Estonia

Dissertation was accepted for the commencement of the degree of Doctor of Philosophy (in Molecular Biology) on 19.06.2017 by the Council of the Institute of Molecular and Cell Biology, University of Tartu

Supervisor: Senior Research Fellow Priit Väljamäe, PhD
Chair of General and Microbial Biochemistry
Institute of Molecular and Cell Biology
University of Tartu, Estonia

Opponent: Associate Professor Kiyohiko Igarashi, PhD
Department of Biomaterial Sciences
Graduate School of Agricultural and Life Sciences
The University of Tokyo, Japan

Commencement: Room No 105, 23B Riia Street, Tartu, Estonia,
on September 20th, 2017, at 12:15.

Publication of this thesis is granted by the Institute of Molecular and Cell Biology, University of Tartu

ISSN 1024-6479
ISBN 978-9949-77-521-7 (print)
ISBN 978-9949-77-522-4 (pdf)

University of Tartu Press
www.tyk.ee

TABLE OF CONTENTS

LIST OF ORIGINAL PUBLICATIONS

The current thesis is based on the following original publications, which will be referred to in the text by their Roman numerals:

I **Velleste R**, Teugjas H, Väljamäe P. (2010). Reducing end-specific fluorescence labeled celluloses for cellulase mode of action. *Cellulose*. 17(1): 125–138.

II **Kont R**, Kari J, Borch K, Westh P, Väljamäe P. (2016). Inter-domain synergism is required for efficient feeding of cellulose chain into active site of cellobiohydrolase Cel7A. *J Biol Chem*. 291(50):26013–26023.

III Kari J, **Kont R**, Borch K, Buskov S, Olsen JP, Cruyz-Bagger N, Väljamäe P, Westh P. (2017). Anomeric selectivity and product profile of a processive cellulase. *Biochemistry*. 56(1):167–178.

My contribution to the articles is as follows:

Ref I Designed and performed the experiments and participated in the data analysis.

Ref II Designed and performed the experiments, analysed the experimental data and participated in writing the manuscript.

Ref III Designed and performed the oligosaccharide degradation and anomer selectivity experiments. Participated in the analysis of experimental data.

LIST OF ABBREVIATIONS

AA	anthranilic acid
AC	amorphous cellulose
BC	bacterial cellulose
rBC	reduced bacterial cellulose
CBH	cellobiohydrolase
CBM	carbohydrate binding module
CBM-linker	CBM together with a linker peptide
CD	catalytic domain
DP	degree of polymerization
$E_{bound\text{-}FA}$	bound enzyme with free active site
$E_{bound\text{-}OA}$	bound enzyme with occupied active site
$E_{bound\text{-}tot}$	total bound enzyme
E_{free}	enzyme free from cellulose
EG	endoglucanase
GH	glycoside hydrolase
IRGs	insoluble reducing groups
k^{obs}	observed catalytic constant
k_{off}	dissociation rate constant
MUL	4-methylumbelliferyl-β-D-lactoside
P^{app}	apparent processivity
P_{odd}	probability of odd-numbered initial cut product
rAC	reduced amorphous cellulose
RG_{tot}	total reducing groups
SEE	substrate exchange experiment
SRGs	soluble reducing groups
T. reesei	*Trichoderma reesei*
*Tr*Ce5A	*T. reesei* endoglucanase Cel5A
*Tr*Ce7B	*T. reesei* endoglucanase Cel7B
*Tr*Cel12A	*T. reesei* endoglucanase Cel12A
*Tr*Cel6A	*T. reesei* cellobiohydrolase Cel6A
*Tr*Cel7A	*T. reesei* cellobiohydrolase Cel7A
W38A	*Tr*Cel7A mutant where tryptophan at the position 38 is substituted with alanine
$W38A_{CD}$	catalytic domain of *Tr*Cel7A mutant where tryptophan at the position 38 is substituted with alanine
WT	wild type *Tr*Cel7A
WT_{CD}	catalytic domain of the wild type *Tr*Cel7A

INTRODUCTION

Cellulose, hemicellulose and lignin are the three main constituents of plant dry matter – so called lignocellulosic biomass – and they are packed into a complex matrix in plant cell walls. Because of its wide abundancy, high annual output and substantial content of carbohydrates, lignocellulosic biomass is a potential raw material for biofuel and chemical production (Lynd *et al.*, 2008). The major component of lignocellulosic biomass is cellulose, which in turn is the most abundant natural polysaccharide. Cellulose is a homopolymer, consisting of glucose whereas hemicellulose is a group of heteropolysaccharides, and lignin is a heterogeneous polyphenolic polymer.

In nature, polysaccharides are converted to monomers by fungi and bacteria. These organisms secrete a myriad of different enzymes to unlock sugars from plant cell walls. The main degraders of cellulose are enzymes referred to as cellulases. Enzymatic hydrolysis is also the preferred route for industrial biomass deconstruction. Because enzymatic reactions are highly selective and require mild operating conditions, they have a potential to provide higher product yields with lower operating costs compared to chemical treatment methods (Wyman, 2001).

In biorefinery, the raw biomass is first pretreated by using physical and/or chemical methods (Yang & Wyman, 2008). The pretreatment is followed by enzymatic hydrolysis, which is conducted with multicomponent enzyme mixtures. In bioethanol production the released sugars are further fermented to ethanol by microorganisms. However, high enzyme loadings are the major operative cost drivers in industrial bioethanol production. Cost reduction of enzyme usage can be achieved through improved enzymatic breakdown of cellulose. For applying knowledge-based strategies like enzyme bioengineering to improve enzymatic breakdown, detailed understanding of molecular mechanisms of enzymatic hydrolysis of cellulose is required.

The first part of my thesis provides a literature overview of cellulose as the substrate and cellulases as the catalytic units. It includes a brief overview of cellulose architecture and cellulose model substrates, which are used in cellulase research, as well as the description of enzymatic machinery needed for efficient degradation of cellulose. I am focusing on enzymatic action of a processive cellobiohydrolase *Tr*Cel7A of a soft rot fungus *Trichoderma reesei*. The second part of the thesis comprises the experimental work done to investigate the structure-function relationships of *Tr*Cel7A by using specific biochemical methods. First, a substrate-labeling method is described that is further applied to measure enzyme's chain end preference, processivity, dissociation and endo-probability (Ref I). The major focus of this study was to reveal the structural elements that are affecting the mode of action of *Tr*Cel7A. The role of Trp38 in the catalytic tunnel as well as the role of carbohydrate binding domain together with a linker in different molecular steps of *Tr*Cel7A action are studied (Ref II). Finally, the basis of diverse initial-cut product pattern of *Tr*Cel7A is investigated (Ref III).

1. REVIEW OF LITERATURE

1.1. Cellulose as the substrate

Lignocellulose is a complex and recalcitrant matrix of different polysaccharides and an aromatic polymer lignin. The main component of lignocellulose is cellulose, representing about 30–50% of plant dry weight (Pauly & Keegstra, 2008). Therefore, cellulose is undoubtedly the most abundant biopolymer on Earth. In nature, cellulose is a substrate for bacterial and fungal cellulolytic enzymes – cellulases. Due to its recalcitrant and heterogeneous structure, cellulose is efficiently degraded only by the cooperation of cellulases with different modes of action.

Cellulose is a homopolymer consisting of β-1,4-linked D-glucose residues in their pyranose forms (Figure 1). As each consecutive glucose residue is rotated by 180° in respect to its neighbours, the minimal repeating unit of cellulose chain is cellobiose (Gardner & Blackwell, 1974). Cellulose chains are straight and unbranched. The chain ends are chemically different from each other and are termed as the reducing and the nonreducing ends. Glucose residue of the nonreducing end is always in the cyclic form. In contrast, the glucose residue in the reducing end is in equilibrium between the cyclic hemiacetal and the open-chain aldehyde form, and the latter can act as a reducing agent. In addition, the cyclic hemiacetal of glucose in the reducing end is in equilibrium between the α- and β-anomeric configurations. The equilibrium mixture of free glucose in an aqueous solution consists of 64% of β-glucose and 36% of α-glucose (Kabayama *et al.*, 1958). To the best of my knowledge there is no experimental data about the anomeric equilibrium of terminal glucose residues in reducing ends of cellulose chains.

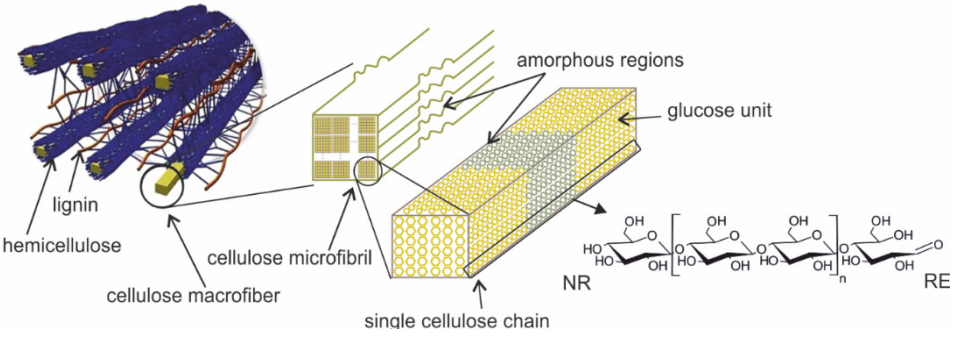

Figure 1. Cellulose is tightly packed into plant cell wall together with other polymers – mainly with hemicellulose and lignin. Cellulose in its native form is mostly crystalline but has also amorphous regions where the crystalline arrangement is disrupted. The higher-order crystalline structures of cellulose such as macrofibers can be divided into smaller building blocks – microfibrils. Microfibrils are formed during the aggregation of co-synthesized cellulose chains *via* hydrogen bonding and van der Waals interactions. Cellulose chains, in turn, consists of glucose units and have two chemically different chain ends: the reducing end (RE) and the nonreducing end (NR). Schematic representation of lignocellulose is reproduced with the permission from Doherty *et al.* (2011).

The length of cellulose chains is expressed in the degree of polymerization (DP), which ranges between 10^2 and 10^4 glucose units (Klemm *et al.*, 2005; Hallac & Ragauskas, 2011). In plants up to 36 parallel-oriented cellulose chains are synthesized simultaneously at cell membrane by rosette-shaped cellulose synthase complexes (Gardner & Blackwell, 1974; Guerriero *et al.*, 2010). The length and the exact amount of the co-synthesized chains is dependent on the source of cellulose. Co-synthesized chains aggregate into crystalline bunches called microfibrils that are constituents of higher-order crystalline structures (Figure 1). Regular and tight noncovalent packaging of cellulose chains is a result of different inter- and intramolecular forces including hydrogen bonding and hydrophobic interactions (Nishiyama *et al.*, 2002; Nishiyama *et al.*, 2003). Additionally, cellulose comprises more disordered amorphous regions. Most probably, the internal strains in the fibre induce microfibrils to tilt and twist, resulting in disorders in cellulose segments (Habibi *et al.*, 2010).The frequency and the extent of these regions are not fully understood. Despite the regions with irregularities, cellulose is considered to be the most recalcitrant native biopolymer. The integrated location of cellulose in plant cell walls and its insoluble crystalline nature hinder its accessibility to cellulolytic enzymes.

1.1.1. Model substrates of native cellulose

To overcome substrate heterogeneity while studying the enzymatic hydrolysis of cellulose, there are plenty of model substrates that can be used instead of native cellulose. The usage of a uniform and well characterized substrate simplifies the interpretation of the results and increases the reproducibility and validity of the experiments. There are several representatives of crystalline and amorphous cellulose (AC) with different structural features such as DP and specific surface area.

Crystalline substrates

The most common crystalline substrates are bacterial cellulose (BC) from *Acetobacterium xylinum* and Avicel – commercially available microcrystalline cellulose made from wood pulp. Avicel is obtained by the controlled hydrolysis of chopped wood pulp with dilute mineral acid. During the treatment, the majority of non-cellulosic polymers and amorphous regions in cellulose structure are removed. Although the DP of cellulose decreases during the treatment, the crystalline parts remain almost intact. The microcrystalline Avicel is nearly pure cellulose with DP of about 200 but it includes a low content of impurities such as hemicellulose and lignin residues (Várnai *et al.*, 2010; Terinte *et al.*, 2011). BC is synthesised as pure cellulose without non-cellulosic polymeric additives, such as hemicellulose and lignin – the common impurities of wood-derived celluloses, and has a DP of few thousands of glucose units. Moderate treatment of BC with HCl results in the formation of bacterial microcrystalline cellulose. This substrate has a lower DP but higher crystallinity

(Väljamäe *et al.*, 1999). Another common substrate representing crystalline cellulose, which is often used to measure total cellulase activity, is Whatman No. 1 filter paper. It is made of cotton cellulose.

Amorphous substrates

Amorphous cellulose is often obtained by the treatment of dry powdered micro-crystalline cellulose (usually Avicel) with phosphoric acid. Phosphoric acid may act as either a dissolving or swelling agent, depending on the severity of the treatment. The transition from swollen cellulose to dissolved cellulose is demonstrated to appear rapidly when the concentration of the phosphoric acid is over 80% (Zhang *et al.*, 2006). Dissolving destroys the crystalline structure of cellulose. Dissolved cellulose is further regenerated by precipitation with water and the structure of regenerated AC is totally disordered. However, after swelling, the structure of the amorphous substrate is not homogeneously amorphous. The fibres of swollen cellulose are partially extended and the surface area of the substrate is increased (Navard & Cuissinat, 2006). Due to the differences in structural properties, the enzymatic accessibility of regenerated AC is higher than that of swollen AC (Zhang *et al.*, 2006).

Soluble substrates

The common soluble polymeric substrates are synthetic cellulose ethers, such as hydroxymethyl and hydroxyethyl cellulose. In these substrates, some of the hydroxyl groups of the glucose residues in cellulose are substituted with corresponding alcoxide groups. These substitutions hinder the substrate from entering to the closed active sites of processive cellobiohydrolases (CBHs). Therefore, these substrates are specific for endo-acting cellulases and are often used to determine the endoglucanase activity of enzymes (Karlsson *et al.*, 2002).

Cellooligosaccharides of DP up to 8 are soluble in water. Oligosaccharides have been widely used to study chain end preference of cellulases (Claeyssens *et al.*, 1989; Bhat *et al.*, 1990; Vrsanska & Biely, 1992; Schou *et al.*, 1993; Barr *et al.*, 1996). Several crystal structures of cellulases are solved in complexes with oligosaccharides (Payne *et al.*, 2015). Oligosaccharides have been used also as substrates to investigate the product pattern and kinetic parameters of the enzymes (Nidetzky *et al.*, 1994; Harjunpää *et al.*, 1996). However, the solubility of cellooligosaccharides decreases with increasing DP, and thus this substrate is not appropriate for studying processivity of cellulases.

The most common low molecular weight model substrates are soluble chromo- and fluorogenic derivatives of lactose and cellobiose. Such substrates are often used for measuring enzyme activity and inhibition. However, these substrates are suitable only for certain cellulases. For example, *Trichoderma reesei* (*T.reesei*) cellulases *Tr*Cel7A and *Tr*Cel7B have 4-methylumbelliferyl-β-D-lactoside (MUL) and para-nitrophenol-β-D-lactoside hydrolysing activity, whereas two other cellulases from *T. reesei*, *Tr*Cel5A and *Tr*Cel6A, do not hydrolyse these substrates.

1.2. Fungal cellulases

The main biomass degraders in nature are fungi and bacteria. They secrete a myriad of different enzymes to deconstruct plant cell wall. Although there is a wide diversity among polysaccharide active enzymes, they mainly belong to the class of glycoside hydrolases (GHs). GHs in turn are distributed into GH families based on the amino acid sequence similarities of their catalytic domains (CDs) (Lombard *et al.*, 2014). GHs employ either retaining or inverting catalytic mechanism (Koshland, 1953). The retaining mechanism involves the formation and the breakdown of a covalent glycosyl-enzyme intermediate. Because of the two consecutive nucleophilic substitutions, the reducing end of the formed product retains its original anomeric configuration. Employing the inverting catalytic mechanism, a single nucleophilic substitution by the attack of a water molecule produces a product with the anomeric configuration different from that of the substrate.

The most studied cellulolytic systems belong to aerobic fungi. The reason may lay in their extracellular secretion, high environmental tolerance and amount of production. Most of the studied fungal cellulases display a two-domain structure, consisting of a CD and a carbohydrate binding module (CBM) that are linked by a glycosylated linker peptide (Figure 2). CBM contributes to the targeting of the enzyme to the substrate (Carrard *et al.*, 2000; McLean *et al.*, 2002; Herve *et al.*, 2010). CBM is also suggested to disrupt non-hydrolytically cellulose surface and deliver the cellulose chain into active site of the enzyme (Din *et al.*, 1994). CBMs are categorized into CBM families (Lombard *et al.*, 2014). CBMs of fungal cellulases belong mostly to the family 1. CBM1 has a hydrophobic and flat binding face that contains three conserved aromatic residues (Kraulis *et al.*, 1989; Nimlos *et al.*, 2012). The flat binding surface is found as a common feature of CBMs that contribute to the binding of carbohydrate-active enzymes to insoluble crystalline substrates such as cellulose and chitin (Boraston *et al.*, 2004). CBM is connected to CD by a glycosylated and flexible linker peptide (Harrison *et al.*, 1998; Stals *et al.*, 2004; Beckham *et al.*, 2010; Sammond *et al.*, 2012; Payne *et al.*, 2013b). The linker keeps the optimal distance between the CD and CBM to achieve the maximal activity on crystalline cellulose (Srisodsuk *et al.*, 1993). The molecular dynamics simulations of the cellulose bound CBHs from the families 6 and 7 showed that the linker can bind to cellulose (Payne *et al.*, 2013b). This observation suggests that the linker may contribute directly to the hydrolysis.

CDs of fungal cellulases display structural conservations and based on structural similarities are clustered into GH families (Lombard *et al.*, 2014). As often obsereved in GHs, CDs of cellulases have an active site with multiple binding subsites for the binding of glycosyl residues of cellulose. The subsites are signed using "–n +n" system from the nonreducing end of the substrate to the reducing end, respectively (Davies *et al.*, 1997). The catalysis occurs in between –1 and +1 subsites. This determines that for the reducing end specific CBHs "+" subsites are product-binding subsites and "–" subsites are substrate-

binding subsites; the situation is opposite in case of the nonreducing end specific CBHs (Figure 2). The active site of cellulases is lined with aromatic residues that contribute to substrate binding by forming hydrophobic stacking interactions with the glucose rings of the cellulose chain (Divne *et al.*, 1998; Taylor *et al.*, 2013).

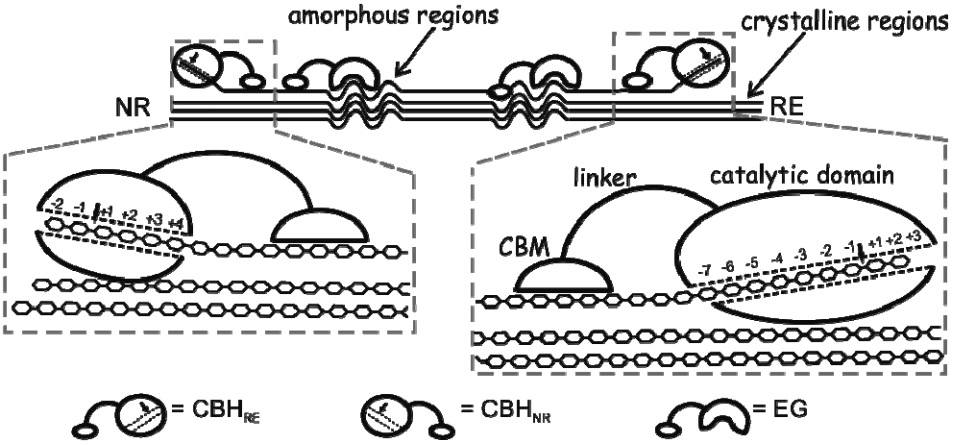

Figure 2. **Schematic representation of CBHs and EGs acting on cellulose.** Cellulases have a two-domain structure. The binding of the enzyme to cellulose is mediated by CBM that is connected to CD via a glycosylated linker peptide. The glycosidic bond hydrolysis is performed by the CD. Reducing end (RE) specific and nonreducing end (NR) specific CBHs, CBH_{RE} and CBH_{NR} respectively, start the hydrolysis preferentially from the opposite chain ends of a cellulose chain. *Tr*Cel6A acting processively from the nonreducing end of cellulose (left), and *Tr*Cel7A acting processively from the reducing end of cellulose (right) are zoomed in. The glucose unit binding sites are numbered and the arrows show the scissile bond. EGs make internal breaks into cellulose chains. Amorphous regions of cellulose are more prone to attacks by EGs due to the disruption of interactive forces between cellulose chains.

Originally, cellulases were divided into three groups based on their mode of action: (i) exo-active processive CBHs; (ii) endoglucanases (EGs) that make internal cuts into cellulose and (iii) cellobiose-active β-glucosidases (Beguin, 1990; Beguin & Lemaire, 1996). The subsequent structural reports have revealed that the active site topology reflects the prevailing hydrolysis mechanism of the enzyme (Kleywegt *et al.*, 1997). So, the enzymes acting mainly on cellulose chain ends in a processive manner have a more closed tunnel-shaped active site, whereas the endoglucanases that make internal breaks into cellulose chains have rather opened cleft-like active sites.

Recently, lytic polysaccharide monooxygenases have been identified as non-hydrolytic cellulose-active enzymes (Vaaje-Kolstad *et al.*, 2010; Quinlan *et al.*, 2011). They use oxidative cleavage mechanism to break glycosidic bonds. These enzymes are grouped into families of auxiliary activities together with other redox enzymes that act in cooperation with other carbohydrate-active enzymes

(Lombard *et al.*, 2014). They increase the availability of the substrate for other cellulases by making chain breaks into crystalline parts of cellulose. During the recent years, lytic polysaccharide monooxygenases have been extensively studied and a rapid progress has been made in understanding their action (Morgenstern *et al.*, 2014).

Cooperated performance of cellulases with different modes of action is shown to be a prerequisite for efficient cellulose degradation (Woodward, 1991; Jalak *et al.*, 2012; Kostylev & Wilson, 2012). The most studied phenomenon is synergism between the endo- and exo-acting cellulases (Wood & McCrae, 1972; Väljamäe *et al.*, 1999; Eriksson *et al.*, 2002). According to the conventional mechanistic interpretation of synergistic action, EGs make internal breaks into cellulose chains in amorphous regions and thereby generate new chain ends for the CBHs action (Wood & McCrae, 1972). This synergistic mechanism was lately complemented with another mechanism (Jalak *et al.*, 2012). Besides generating starting points for CBHs, the internal breaks generated by EGs were proposed to act also as "escape routes" for processive CBHs to avoid stalling at the obstacles (Igarashi *et al.*, 2011; Jalak *et al.*, 2012).

1.2.1. *Trichoderma reesei* cellulases

A soft rot fungus *Trichoderma reesei* (teleomorph *Hypocrea jecorina*) is the main cellulase producer for industrial applications. Since its isolation (the QM6a strain) and identification in 1944 from US Army tent canvas in the Solomon Islands, the strain has been extensively studied and improved. A landmark in the development of more efficient cellulase produces was a carbon catabolite depressed hypercellulolytic strain RUT-C30. Furthermore, the modern industrial strains with considerably higher yields of protein production (more than 100 g/l) are all descendants of the RUT-C30 strain (Peterson & Nevalainen, 2012). For efficient cellulose degradation *T. reesei* produces at least 2 CBHs, 6 EGs, 7 β-glucosidases and 2 lytic polysaccharide monooxygenases (Lombard *et al.*, 2014).

Cellobiohydrolases

The CBHs *Tr*Cel7A and *Tr*Cel6A belong to the GH families 7 and 6, respectively. *Tr*Cel7A is the key enzyme in cellulose degradation, representing about 60% of total enzymes secreted by the fungus. *Tr*Cel7A acts processively by starting the hydrolysis from the reducing end of a cellulose chain (Imai *et al.*, 1998; Nutt *et al.*, 1998). It employs the retaining catalysis mechanism (Knowles *et al.*, 1988; Claeyssens *et al.*, 1990). *Tr*Cel7A is not a true exo-enzyme, it harnesses the endo-mode initiation mechanism in parallel (Kurašin & Väljamäe, 2011). Another CBH, *Tr*Cel6A is shown to start hydrolysis from the non-reducing end of the cellulose chain (Chanzy & Henrissat; Nutt *et al.*, 1998), and by applying the inverting catalysis mechanism liberates α-cellobiose as the main hydrolysis product (Knowles *et al.*, 1988; Claeyssens *et al.*, 1990; Koivula *et*

al., 2002). The active site tunnel of *Tr*Cel6A is 20 Å long and accommodates at least 6 glucose residues of the cellulose chain (binding at subsites +4 to –2, Figure 2) (Koivula *et al.*, 1998). Based on structural differences between *Tr*Cel7A and *Tr*Cel6A and remarkable flexibility of closing loops of the active site of *Tr*Cel6A (Zou *et al.*, 1999), *Tr*Cel6A is proposed to be less processive and to have higher inclination for endo-initiations than *Tr*Cel7A (Boisset *et al.*, 2000). However, the suggestions based on structural differences do not coincide with experimental measurements. By single-molecule imaging with high-speed atomic force microscopy, the processivity of *Tr*Cel6A was measured approximately 3 times higher than that of *Tr*Cel7A in the same system (Nakamura *et al.*, 2016). In addition, there are few studies, where the endolytic activity of *Tr*Cel6A is measured and, surprisingly, found lower than that of *Tr*Cel7A (Irwin *et al.*, 1993; Badino *et al.*, 2017).

Endoglucanases TrCel7B, TrCel5A and TrCel12A

The most abundant and well-studied EGs of *T. reesei* are *Tr*Cel7B, *Tr*Cel5A and *Tr*Cel12A. All three EGs exhibit retaining, double displacement catalytic mechanism. *Tr*Cel5A forms up to 55% of the total EG activity of the organism (Suominen *et al.*, 1993), and it is also major EG component of commercial enzyme mixtures for biomass saccharification. (Davies *et al.*, 1998). The second abundant EG is *Tr*Cel7B that forms 25% of total EG activity of *T. reesei* (Suominen *et al.*, 1993).

Compared to the active site of GH7 CBH *Tr*Cel7A, several loops are absent from both ends of the active site of *Tr*Cel7B, generating a more open cleft-like substrate binding area (Kleywegt *et al.*, 1997). These differences in loops are probably responsible for the endo-initiation mechanism of *Tr*Cel7B and its decreased processivity compared to that of *Tr*Cel7A (Taylor *et al.*, 2013). Both enzymes have at least nine binding subsites, 7 (–7 to –1) for the substrate binding and at least 2 (+1 and +2) for the product binding. The energy calculations revealed the dissimilarities between *Tr*Cel7A and *Tr*Cel7B in enzyme-ligand binding interactions and hydrogen bonding pattern in all binding subsites, except in subsiste –2 (Taylor *et al.*, 2013). The binding in this subsite is probably equally important in both enzymes for the catalytically active enzyme-substrate complex formation.

*Tr*Cel12A is smaller than *Tr*Cel7B and *Tr*Cel5A, and is one of the three cellulases of *T.reesei* lacking the CBM (Hakansson *et al.*, 1978; Foreman *et al.*, 2003). *Tr*Cel12A is expressed at relatively low level, constituting less than 0.5% of the total culture medium protein content (the levels of *Tr*Cel5A and *Tr*Cel7B are more than tenfold higher) (Ülker & Sprey, 1990). *Tr*Cel12A has a cleft-like active site that is suggested to accommodate at least six glucose residues of the cellulose chain (Sandgren *et al.*, 2001). *Tr*Cel12A is reported to participate in the extension of plant cell walls (Yuan *et al.*, 2001; Park & Cosgrove, 2012).

1.2.2. *Tr*Cel7A

The structure of *Tr*Cel7A was presented in 1994 as the first protein structure from GH family 7 (Divne *et al.*, 1994). The active site of *Tr*Cel7A is 50 Å long and has 10 subsites (from –7 to +3, Figure 2) for the binding of glucose units. Subsite +3 is filled only in case the product is longer than cellobiose (Divne *et al.*, 1998). Catalysis by *Tr*Cel7A is mediated by two-step retaining mechanism (Knowles *et al.*, 1988; Claeyssens *et al.*, 1990). Therefore, the main *Tr*Cel7A product is β-cellobiose. Glucose and cellotriose are also released, but in smaller amounts (Nidetzky *et al.*, 1994; Medve *et al.*, 1998; von Ossowski *et al.*, 2003). The conserved catalytic triad of GH7 enzymes comprises two Glu residues and an Asp: Glu212, Glu217 and Asp214, respectively, in the case of *Tr*Cel7A. Glu217 is identified as the catalytic acid/base and Glu212 as the nucleophile, Asp214 forms a hydrogen bond with Glu212 and promotes the catalysis (Divne *et al.*, 1994; Stahlberg *et al.*, 1996). Both glutamate mutations to glutamine were shown to remove the catalytic activity of the enzyme on crystalline substrates, and the mutation of aspartate to asparagine diminished the activity moderately (Stahlberg *et al.*, 1996).

The active site of *Tr*Cel7A is lined with four aromatic residues: Trp40, Trp38, Trp367 and Trp376 (shown on Figure 5). These residues determine the main enzyme-substrate interactions at the binding subsites –7, –4, –2 and +2, respectively (Taylor *et al.*, 2013). In these subsites aromatic residues form face to face hydrophobic stacking interactions with the corresponding glucosyl moieties in the cellulose chain (Divne *et al.*, 1998). There are several experimental proofs about negative effects of replacements of aromatic residues with non-aromatic ones on the binding and activity of *Tr*Cel7A. Trp40 at the entrance of the binding tunnel of *Tr*Cel7A was shown important for the chain feeding and for the initiation of processive cellulose hydrolysis on a crystalline substrate (Igarashi *et al.*, 2009; Nakamura *et al.*, 2013). The substitution of Trp38 with alanine decreased the binding affinity of *Tr*Cel7A to cellulose, but, in contrast, had a positive effect on the initial rates of hydrolysis at high substrate loads (Kari *et al.*, 2014). Trp367 and Trp376 are suggested to be important for the catalysis by stabilizing the enzymes-substrate complex (Payne *et al.*, 2011; Knott *et al.*, 2014a), but to my knowledge, substitution mutations of these residues have not been described to date.

1.2.3. Molecular steps of cellulose hydrolysis by *Tr*Cel7A

A full processive cycle of *Tr*Cel7A on cellulose is a multi-step process. In literature, different dissections of the processive cycle can be found depending on the focus of the study. Here, the processive cycle of *Tr*Cel7A is dissected into three steps: feeding, processive hydrolysis and dissociation (Figure 3). The feeding includes adsorption of the enzyme to the surface of substrate, recognition of the reducing end of a cellulose chain and its initial sliding into the active site until the subsite –1. The feeding can be characterized kinetically

by the on-rate (k_{on}). During the hydrolysis, the product subsites (+1 and +2) are filled and the Michaelis complex is formed. Upon the hydrolysis of the glycosidic bond and expulsion of the cellobiose product, the reducing end of cellulose chain is in the subsite –1 and the steps of processive hydrolysis are repeated. The processive hydrolysis is characterized kinetically by the processivity number and the catalytic rate constant (k_{cat}). The processive cycle ends with dissociation that is governed by the dissociation rate constant (k_{off}) of the enzyme.

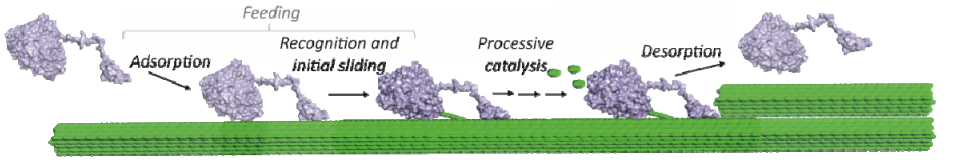

Figure 3. Elementary steps of the full processive cycle of *Tr*Cel7A. Enzyme adsorption, recognition and initial sliding are collectively referred to as feeding. The feeding is followed by processive catalysis during which the enzyme performs several consecutive catalytic acts. The repeated unit of the processive catalysis consists of three main elementary steps: productive complex formation, the hydrolysis of glycosidic bond and expulsion of cellobiose. Processive catalysis is terminated by the encounter of an obstacle and dissociation of the enzyme. Figure 3 is adapted from Kont *et al*, 2016.

Feeding

Binding of the enzyme to cellulose surface is a prerequisite for the enzymatic catalysis. According to a two-step binding model, first the enzyme adsorbs to cellulose *via* CBM, which is followed by the recognition of the cellulose chain end at the entrance region of the active site of the CD (Nakamura *et al.*, 2013; Cruys-Bagger *et al.*, 2016). CBM facilitates the enzyme binding to cellulose having higher affinity towards crystalline substrates (Guo & Catchmark, 2013). The primary role of CBM is in increasing the local concentration of the enzyme on cellulose surface and its effect diminishes with increasing substrate loads (Ståhlberg *et al.*, 1991; Cruys-Bagger *et al.*, 2013b; Várnai *et al.*, 2013).

The recognition and sliding of the cellulose chain into the active site is proposed by computational studies to be guided by the aromatic residues lining the active site (Knott *et al.*, 2014a). However, only the importance of Trp40 is experimentally approved. In a visualization study using high-speed atomic force microscopy, many *Tr*Cel7A molecules with Trp40 substituted with an alanine were inefficient in complexation with crystalline cellulose (Igarashi *et al.*, 2009). Further investigations revealed that Trp40 participates in the anchoring of cellulose chain end to the active site by increasing the affinity of the entrance region and its significance depends on the length of the available chain end (Nakamura *et al.*, 2013).

*Tr*Cel7A is suggested to be able to start the hydrolysis also without initial sliding. Although *Tr*Cel7A is classically considered as an exo-active reducing end specific CBH, its capability to start the hydrolysis in endo-fashion is also

demonstrated. Moreover, about half of the initiations of *Tr*Cel7A on BC were reported to be of endo-type (Kurašin & Väljamäe, 2011). The mechanism of endo-attacks is largely speculative, but it is proposed that the active site opens up by the movement of the loops that usually form the closed tunnel, and enables the direct binding of cellulose chain over the active site without initial sliding (Stahlberg *et al.*, 1993).

Processive catalysis

The processive cycle of *Tr*Cel7A is thoroughly studied and described step by step by applying different approaches. Crystal structures together with molecular simulations have helped to get a detail understanding of the changes in carbohydrate-protein interactions during the catalytic cycle (Knott *et al.*, 2014b). The first step of the processive catalysis is the second slide where the chain advances one cellobiose unit further and occupies the product subsites, forming thus the productive enzyme-substrate complex. The productive complex represents the state where the enzyme is bound to the substrate so that the cellulose chain end is in the product-binding site and the oxygen atom of scissile bond is in the correct orientation for the catalysis. After the formation of a productive complex, the glucose residues in the active site are in their chair conformation. The following catalytic activation distorts the glucose ring in subsite –1 into envelope conformation, whereby anomeric carbon moves toward the nucleophile (Glu212) and the Michaelis complex is formed. In the first chemical step of retaining hydrolysis, termed enzyme glycosylation, cellobiose is cleaved from the reducing end, whereas the rest of the cellulose chain remains covalently bound to the nucleophile. Although there are some contradictions between the results of different computational studies, it is generally thought that the glycosylation step is the rate- limiting step of the catalytic cycle of *Tr*Cel7A (Knott *et al.*, 2014a; Knott *et al.*, 2014b; Payne *et al.*, 2015). The crystal structures of the Michaelis complex and the glycosyl-enzyme intermediate of *Tr*Cel7A (Knott *et al.*, 2014b) suggest that, the cellobiose product may be in two different binding modes. This finding supports the results of computer simulation studies that after glycosylation the cellobiose product is shifted slightly further (+1 and +2 subsites remain still occupied) and assists the nucleophilic water during the second catalytic step, termed deglycosylation. During deglycosylation, the glycosyl-enzyme intermediate is hydrolysed and the cellobiose leaves the active site. The enzyme continues with the processive run by moving one cellobiose unit further on a cellulose chain to form a new productive complex.

Following the cellobiose product formation during cellulose hydrolysis by *Tr*Cel7A it can be seen that the hydrolysis rate is maximal at the initial stage of hydrolysis (first 10–20 s), after that the rate retards rapidly (Karuna & Jeoh, 2017). At the initial stage, the binding through the active site is suggested to be productive. However, there is no direct method to evaluate the productive enzyme complexes on cellulose. Still, by measuring the inhibition of reporter molecule (like MUL) hydrolysis by cellulose is possible to quantify the active

site bound enzyme on cellulose ($E_{bound\text{-}OA}$). As MUL binds to the subsites –2 to +2 of *Tr*Cel7A, the method does not permit to distinguish between real productive complexes and complexes were cellulose chain end is just further from subsite –3. Therefore, only this initial stage is suitable for calculating the k_{cat} value as a ratio of the rate of cellobiose formation to the concentration of the active site bound enzyme, $k_{cat}=v_{CB}/[E]_{bound\text{-}OA}$ (Jalak & Väljamäe, 2010; Karuna & Jeoh, 2017). Jalak and Väljamäe measured the observed catalytic constant ($k^{obs}=v_{CB}/[E]_{bound\text{-}OA}$) in time and reported that, indeed, the k^{obs} started to decrease rapidly, whereas the concentration of the enzyme bound *via* the active site remained unchanged. This finding supported the obstacle model, whereby the enzyme molecules move with the rate determined by the k_{cat} until they encounter steric obstacles that hinder the further movement. The enzymes stall most probably in nonproductive complexes with cellulose chain end in subsite –1. However, since it is not possible to distinguish these complexes from productive complexes, the concentration of the active site bound enzyme remains unchanged (Jalak & Väljamäe, 2010).

Plausibility of the obstacle model is also supported by the observations that the processivity values measured for *Tr*Cel7A are at least two orders of magnitude lower than the processivity potential (intrinsic processivity) of the enzyme (Kurašin & Väljamäe, 2011). The concept about steric obstacles was also supported by the innovative study with high-speed atomic force microscopy where the movement of CBHs on crystalline cellulose was monitored (Igarashi *et al.*, 2009; Igarashi *et al.*, 2011). Two populations of *Tr*Cel7A were detected: one population was moving and the other was stalled. The stalled enzymes were observed to accumulate behind steric obstacles. Furthermore, in some cases the joined enzyme molecules collectively peeled off the obstacle and moved on. Later, it was proposed that the collective action of the enzyme molecules with strong binding potential at unoccupied product-binding subsites forms a cumulative force to remove the obstacles from their path (Kurašin *et al.*, 2015). If the cumulative force is not sufficient to get rid of the obstacle, the enzyme will stay stalled until the dissociation.

Dissociation

The dissociation of the stalled enzyme is determined by the off-rate constant. It is now widely accepted that the dissociation is the rate limiting step of the overall processive cycle of individual *Tr*Cel7A and the recruitment of the enzyme is governed by the off-rate constant (Jalak & Väljamäe, 2010; Kurašin & Väljamäe, 2011; Cruys-Bagger *et al.*, 2012a; Cruys-Bagger *et al.*, 2013a; Cruys-Bagger *et al.*, 2013b; Kari *et al.*, 2014). According to the obstacle model, the obstacle-free path for the movement limits the length of the processive run of the enzyme. Provided that the dissociation is slower than the processive run, the overall rate of the hydrolysis by individual CBHs after the initial burst is governed by the off-rate constant and by the length of the obstacle-free path (n) ($k^{obs}\approx k_{off}$*n) (Jalak & Väljamäe, 2010).

Numerous crystal structures of cellulases in parallel with computational and experimental studies have shed light on connections between the structural and kinetic properties of cellulases. Slower dissociation and decreased hydrolytic activity on amorphous and soluble substrates are shown to be the price of high processivity (Nakamura *et al.*, 2014). EGs with more open active sites and, thus, weaker binding to the substrate have decreased processive ability and significantly higher dissociation rates compared to processive CBHs (Kurašin & Väljamäe, 2011; Taylor *et al.*, 2013). Similar tendency has been also found among CBHs with different active site architectures. Cel7D from fungus *Phanerochaete chrysosporium* has a more open active site and hence decreased processive ability and about fourfold higher off-rate value than *Tr*Cel7A (Kurašin & Väljamäe, 2011; Nakamura *et al.*, 2014).

1.2.4. Product inhibition of *Tr*Cel7A

Several computational studies have shown that glucose units bind to the product-binding subsites more tightly than to the substrate-binding subsites (Bu *et al.*, 2011; Bu *et al.*, 2012; Payne *et al.*, 2013a; Knott *et al.*, 2014a). The strong binding of glucose units in the product binding subsites +1 and +2 of *Tr*Cel7A is suggested to be the driving force to advance cellulose chain by one cellobiose unit further during the processive hydrolysis (Payne *et al.*, 2015). An adverse side effect of the strong binding in the product binding subsites is the concomitant product inhibition. Although *Tr*Cel7A is inhibited by both main hydrolysis products, cellobiose and glucose, cellobiose is shown to be the stronger inhibitor of the enzyme (Murphy *et al.*, 2013; Teugjas & Väljamäe, 2013).

The product inhibition of *Tr*Cel7A is often studied with soluble fluoro- or chromogenic low molecular weight model substrates (van Tilbeurgh & Claeyssens, 1985; Voutilainen *et al.*, 2008; Teugjas & Väljamäe, 2013). The product inhibition mechanism measured using soluble substrates is reported as competitive and occurs as a competition between the product and the substrate for the binding to the product-binding subsites (Voutilainen *et al.*, 2008). Although widely used, the inhibition type and strength measured on low molecular weight model substrates do not correlate with these measured on insoluble polymeric substrates. Moreover, the differences in inhibition strength measured on different types of substrates are not constant among the cellulases (Gruno *et al.*, 2004; Teugjas & Väljamäe, 2013). For *Tr*Cel7A, the inhibition constant of cellobiose measured on BC is an order of magnitude higher than that measured on low molecular weight model substrate (Teugjas & Väljamäe, 2013). The similar trend holds also for glucose as well as gluco- and xylooligosachharide inhibition (Baumann *et al.*, 2011; Kont *et al.*, 2013). Therefore, native cellulosic substrates should be used for selecting cellulases for lignocellulose deconstruction (Teugjas & Väljamäe, 2013). However, the product inhibition on cellulose is found more complex and there are several contradicting results concerning the exact inhibition mechanism (Howell & Stuck,

1975; Howell, 1978; Lee & Fan, 1982; Gruno *et al.*, 2004; Andric *et al.*, 2010a; Bezerra *et al.*, 2011; Jalak *et al.*, 2012). Recently, it has been found that product inhibition of *Tr*Cel7A in hydrolysis of cellulose matches well with the noncompetitive inhibition mechanism (Kuusk *et al.*, 2015; Olsen *et al.*, 2016). The addition of the accumulation of the stalled enzyme-substrate complexes into the model of product inhibition of *Tr*Cel7A accounted well for the differences in the type and strength of inhibition of *Tr*Cel7A measured on polymeric versus low molecular weight substrates (Kuusk *et al.*, 2015).

Several studies have tried to shed light to the basis of the strong product inhibition of *Tr*Cel7A. Comparing *T. reesei* cellulases and the processive CBH Cel7D from *Phanerochaete chrysosporium*, the strongest cellobiose inhibition is measured for *Tr*Cel7A – the enzyme with the "most closed" active site (von Ossowski *et al.*, 2003; Gruno *et al.*, 2004; Teugjas & Väljamäe, 2013). Probably more open active site is more extensively solvated and therefore electrostatic interactions between the protein and the carbohydrate are disrupted more easily (von Ossowski *et al.*, 2003; Ubhayasekera *et al.*, 2005). Several structural elements of the active site have been identified to be linked with strong product inhibition of *Tr*Cel7A. For example, the weaker binding of cellobiose to *Tr*Cel7A is achieved by disrupting the intermolecular hydrogen bonding interactions between the cellobiose and the product-binding subsites of the enzyme (von Ossowski *et al.*, 2003). The inflexible exo-loop that closes the active site tunnel of *Tr*Cel7A is also suggested to contribute to strong product inhibition (Textor *et al.*, 2013).

GH7 cellulases are key enzymes in commercial cellulase mixtures and it is relevant to achieve high product yields of cellulose decomposition. To relieve product inhibition during cellulose degradation, most commonly β-glucosidases are added to the reaction mixture. β-glucosidases convert cellobiose into two molecules of glucose, which is by two orders of magnitude weaker inhibitor of *Tr*Cel7A than cellobiose (Murphy *et al.*, 2013; Teugjas & Väljamäe, 2013). There are also other strategies developed for industrial use such as product removal by membrane filtration or simultaneous saccharification and fermentation process (Andric *et al.*, 2010b). In the latter case, cellulases convert insoluble substrate to soluble sugars, which are simultaneously utilized by fermenting organisms (yeast) in the medium.

2. AIMS OF THE STUDY

Processive cellobiohydrolases are the main workhorses of cellulolytic systems and are thereby the primary targets for protein engineering to increase the efficiency of enzymatic conversion of cellulose. Therefore, the focus is directed increasingly toward molecular details of processive action of cellulases.

The structural and computational studies have revealed distinct molecular steps and a dynamic network of interactions in processive cellulose hydrolysis by cellobiohydrolases from the glycoside hydrolase family 7. The processive cycle of cellulose hydrolysis by CBHs includes the following steps: adsorption, substrate recognition, cellulose chain sliding to the active site, productive complex formation, processive catalysis and dissociation. However, the biochemical studies on structure-function relationships are still scarce.

As cellulases function on a solid-liquid interface of a recalcitrant substrate, we elaborated a specific substrate labeling method to study their action (Ref I). Both, Ref II and Ref III focus on particular cellulase-cellulose interactions that are important for enzyme-substrate complex formation and processive performance of *Tr*Cel7A.

3. METHODOLOGICAL CONSIDERATIONS

A detailed description of the used methods is provided in publications added to the thesis; only the specific substrates and methods developed by us to study the kinetics of CBHs on polymeric substrates are described here.

3.1. Cellulosic substrates

Avicel is a wood derived cellulose. Because of its crystalline structure, Avicel is an appropriate substrate to study the action of processive CBHs. The main advantage of Avicel is its commercial availability that increases the reproducibility of experiments.

Bacterial cellulose (BC) forms a stable suspension in aqueous medium and has a degree of polymerization close to that of native cellulose. Therefore, BC is a common model substrate to study the processive performance, chain end preference, processivity, and rate constants of different molecular steps of CBHs.

Amorphous cellulose (AC) has a disordered structure without crystalline regions. AC has the highest binding capacity among cellulosic substrates. Therefore, AC is an appropriate substrate to study the binding and activity of enzyme variants with low binding efficiency. It is possible to reveal the effect of substrate properties on the action of enzyme when the hydrolysis is performed with AC and crystalline cellulose in parallel.

Fluorescence-labeled cellulose is a cellulose with available reducing ends labeled with fluorescent amines via reductive amination. Such labeling enables the quantification of reducing groups by sensitive fluorescent detection. Also, it is possible to quantify the amount of released end label. If the reaction conditions are selected so that the probability of the repeated attacks on reducing ends of the same cellulose chain is negligible, the released end label represents the amount of initial attacks of the enzyme from the reducing ends (Kurašin & Väljamäe, 2011). Fluorescence labeling of polymeric carbohydrates has been used for studying endo-mode probability, processivity, and off-rate of both, cellulases (Kipper *et al.*, 2005; Kurašin & Väljamäe, 2011) and chitinases (Kurašin *et al.*, 2015).

^{14}C-labeled cellulose – is a ^{14}C-labeled analogue of BC, where ^{14}C is incorporated uniformly into the cellulose. As the detection of the radioactive product formation is very sensitive, this substrate is appropriate for measuring the hydrolysis rates during the initial rapid phase of hydrolysis. ^{14}C-labeled cellulose is also used as a substrate to measure the kinetic parameters and inhibition of cellulases (Jalak *et al.*, 2012; Teugjas & Väljamäe, 2013)

Reduced cellulose is a cellulose where aldehyde groups of reducing ends are converted to sugar alditols. Sugar alditols are not reactive in cellulase assays that chemically quantify reducing groups. Therefore, by performing enzymatic hydrolysis on reduced cellulose, it is possible to measure the amount of newly generated reducing groups during cellulose hydrolysis. If the hydrolysis is performed under conditions where the probability of repeated initiations from reducing ends of the attached chains is negligible, the amount of new reducing groups on cellulose equals to the number of initiations employed by the enzyme. Reduced cellulose has been used as a substrate for measuring processivity, off-rate, and endo-mode initiations of cellulases (Kurašin & Väljamäe, 2011).

3.2. Measuring apparent processivity and the rate constant of the initiation of processive run

The method was developed by Kurašin and Väljamäe (2011) to measure the processivity of cellulases on cellulosic substrates. Apparent processivity (P^{app}) is defined as an average number of catalytic acts (N_{catal}) performed per number of initiations of processive runs (N_{init}) on a polymer (Equation 1).

$$P^{app} = \frac{N_{catal}}{N_{init}} = \frac{[IRG]+[SRG]}{[IRG]} = \frac{RG_{tot}}{IRG} \qquad \text{Eq. 1}$$

Upon enzymatic hydrolysis of reduced cellulose, two different types of reducing groups are generated: (i) soluble reducing groups (SRGs, reducing ends of released soluble products) and (ii) insoluble reducing groups (IRGs, reducing ends of residual insoluble cellulose). The hydrolysis is performed under the conditions where the probability of repeated attacks on reducing ends of the same cellulose chain is negligible. After separation of residual cellulose by centrifugation, the concentration of SRGs is measured in the supernatant. SRGs were measured using 3-methyl-2-benzothiazolinone hydrazone hydrochloride method (Ref II) (Horn & Eijsink, 2004). The concentration of IRGs on residual cellulose is measured by the fluorescence labeling. The former reducing ends of reduced cellulose cannot be labeled with fluorescent amines whereas the enzymatic attacks, either reducing end exo- or endo-specific, generate new IRGs that can be subjected to reductive amination. We used the fluorescence labeling of IRGs with AA (Ref II). The fluorescence of incorporated AA was measured after solubilisation of AA-labeled cellulose by incubating with a crude mixture of cellulases.

An average number of catalytic acts can be found as a total concentration of reducing groups (RG_{tot}) generated during the hydrolysis of reduced cellulose. RG_{tot} can be found as a sum of IRGs and SRGs. Plotting the data in coordinates RG_{tot} *versus* IRGs, the slope of the linear regression line is equal to P^{app} value.

The rate constant of the production of IRGs (k_{IRG}) on reduced cellulose can also be used as a measure of k_{off} of the enzyme. k_{IRG} can be found by using the following relationship:

$$k_{off} = k_{IRG} = \frac{v_{IRG}}{[E]_{bound-OA}} \quad \text{Eq. 2}$$

In Equation 2, v_{IRG} is the rate of the generation of IRGs and $[E]_{bound\text{-}OA}$ stands for the concentration of the enzyme bound to cellulose through the active site. When expressed in this way, k_{off} represents the dissociation of the cellulose chain from the enzyme active site (Ref II).

3.3. Measuring the off-rate of *Tr*Cel7A by substrate exchange experiment

Substrate exchange experiment (SEE) method was originally developed to measure the off-rates of chitinases (Kurašin *et al.*, 2015). We adapted the method to measure the off-rate of *Tr*Cel7A and its variants (Ref II). In SEE, the total dissociation of the enzyme is measured. Independent of the rate- limiting step of enzyme recruitment, the off-rate is found in SEE as an exchange rate of the enzyme between a nonlabeled substrate (substrate of interest) and a ^{14}C-labeled reference substrate. For measuring the off-rate of *Tr*Cel7A, Avicel was used as the substrate of interest and ^{14}C-labeled AC as the reference substrate (Ref II). The enzyme was first pre-incubated with Avicel. After defined time the reaction was supplemented with ^{14}C-labeled AC and the release of ^{14}C-labeled product in time was followed by measuring radioactivity. For straightforward interpretation of the results, both substrates must be used in concentrations that are saturating for the enzyme. For constructing the reference curves, both substrates were mixed together before the addition of the enzyme. Reference curves were analysed by nonlinear regression analysis according to Equation 3.

$$[(^{14}C)cellobiose] = At^b \quad \text{Eq. 3}$$

[(^{14}C)cellobiose] is the concentration of the ^{14}C-labeled cellobiose, t is time and A and b are empirical constants (Kostylev & Wilson, 2013). Data from the time curves of SEE were analysed using nonlinear regression according to Equation 4:

$$[(^{14}C)cellobiose] = A\left(1 - e^{-k_{off}t}\right)t^b \quad \text{Eq. 4}$$

In the latter analysis, the value of b was fixed to the value found from the analysis of the reference curve, k_{off} and A were let free.

3.4. Measuring the total and active site mediated binding of *Tr*Cel7A to cellulose

*Tr*Cel7A can bind to cellulose using different binding modes. It is possible to measure experimentally (i) the total concentration of enzyme bound to cellulose ($[TrCel7A]_{bound\text{-}tot}$) and (ii) to discriminate between two different binding modes of the bound enzyme: the bound enzyme with the active site free for MUL hydrolysis ($TrCel7A_{bound\text{-}FA}$) and the bound enzyme with the active site occupied by cellulose ($TrCel7A_{bound\text{-}OA}$) (Jalak & Väljamäe, 2010, 2014). $TrCel7A_{bound\text{-}FA}$ consists of populations of bound enzyme with the cellulose chain occupying the binding subsites up to –3 whereas the binding subsites –2 to +1 are free, and the enzyme can hydrolyse MUL. However, when the enzyme is bound to the cellulose in a way that cellulose chain occupies the binding subsite –2, the enzyme cannot hydrolyse MUL and is referred to as $TrCel7A_{bound\text{-}OA}$.

$[TrCel7A]_{bound\text{-}tot}$ can be found as the difference between the total concentration of *Tr*Cel7A in the experiment and the concentration of the enzyme free from cellulose ($[TrCel7A]_{free}$). $[TrCel7A]_{free}$ can be found by measuring the MUL hydrolysing activity in the filtrate after separating cellulose with the bound enzyme by filtration.

If $[TrCel7A]_{bound\text{-}tot}$ is known, the two different enzyme populations of bound enzyme can be distinguished by measuring the initial rates of MUL hydrolysing activity in the presence of cellulose. $[TrCel7A]_{bound\text{-}OA}$ can be found as the difference between total concentration of *Tr*Cel7A and the concentration of the enzyme with free active site $[TrCel7A]_{FA}$. $[TrCel7A]_{FA}$ can be found by measuring the inhibition of MUL hydrolysing activity by cellulose, using the standard curves made without presence of cellulose. $[TrCel7A]_{bound\text{-}FA}$ can be found as the difference between $[TrCel7A]_{bound\text{-}tot}$ and $[TrCel7A]_{bound\text{-}OA}$.

3.5. Determination of anomer selectivity in binding subsite +2 of *Tr*Cel7A

The method is based on measuring the inhibition of *Tr*Cel7A catalysed hydrolysis of fluorescent reporter molecule MUL by different anomers of cellobiose (Ref III). It has been shown that cellobiose is a competitive inhibitor of MUL hydrolysis (Voutilainen *et al.*, 2008). It is also well known that the strongest binding of cellobiose is at product-binding subsites (+1 and +2) of the enzyme (von Ossowski *et al.*, 2003; Bu *et al.*, 2011). If the binding at subsite +2 is anomer-selective, the strength of cellobiose inhibition should depend on the anomeric form of bound cellobiose. Hence, the inhibition of MUL hydrolysis by cellobiose was measured using initially either β- or α-anomeric form of cellobiose. Upon preparing the fresh solution of cellobiose in either anomeric form, it starts to establish an equilibrium mixture of two anomers (64% $cellobiose_{\beta}$ vs. 36% $cellobiose_{\alpha}$) governed by the rate constant of mutarotation (Kabayama *et al.*, 1958). To reveal the dependence of the inhibition strength of

*Tr*Cel7A catalysed hydrolysis of MUL on the anomeric configuration of cellobiose, the inhibition of MUL hydrolysis was measured using cellobiose preparations of different age.

The solution of cellobiose$_\beta$ was prepared by rapid dissolving of the solid powder of cellobiose$_\beta$. The moment of the dissolution was taken as the zero timepoint for the aging of the preparation. For cellobiose$_\alpha$ preparation, hydrolysis of cellulose was performed with inverting enzyme *Tr*Cel6A. The reaction was conducted at 0 °C to avoid mutarotation of the released cellobiose$_\alpha$. The moment of separation of supernatant from the residual cellulose after the hydrolysis was taken as the zero timepoint for the aging of the cellobiose$_\alpha$ preparation. The binding constants for cellobiose$_\alpha$ and cellobiose$_\beta$ were found from the dependence of the inhibition strength of the corresponding cellobiose preparation (Ref III, Eq. 1 & 2).

4. RESULTS AND DISCUSSION

4.1. Reducing end specific fluorescence labeling of cellulose (Ref I)

Polymer-active enzymes can be classified according to their mode of action in terms of attacking cellulose chain. According to the conventional classification, cellulases are divided into endo-acting EG-s and exo-acting CBHs. CBHs are further classified as reducing end or nonreducing end acting enzymes. The conventional method for assessing chain end preference of CBHs relies on measuring the product pattern of the hydrolysis of end-labeled oligosaccharide substrates (Claeyssens *et al.*, 1989; Bhat *et al.*, 1990; Vrsanska & Biely, 1992; Schou *et al.*, 1993; Barr *et al.*, 1996; Tuohy *et al.*, 2002; Zverlov *et al.*, 2002; Aronson *et al.*, 2003). Also the hydrolysis of oligosaccharides with precise analysis of the anomeric composition of the products has been used (Harjunpää *et al.*, 1996; Aronson *et al.*, 2003; Honda *et al.*, 2008). However, numerous studies have pointed out that the mode of action of enzymes on oligosaccharidic substrates may differ from that employed on polymeric substrates. The simplest approach to assess the mode of action on a polymeric substrate is to use an end-labeled polymeric substrate. Since the nonreducing end of cellulose chain has no specific reactive site, only the reducing-end specific labeling of cellulose is attainable. For using cellulose as a substrate in studies of the action mode of cellulases, at least four conditions must be met in reducing-end labeling of cellulose: (i) the labeling reaction must have very high selectivity for the terminal aldehyde, (ii) the labeling has to be quantitative, (iii) the label must enable a very sensitive detection, (iv) the label must not alter the mode of action of the enzyme. The reducing end specific labeling of cellulose can be achieved through nonradioactive (Arai *et al.*, 1989; Kipper *et al.*, 2005) or radioactive reduction of C1 aldehyde (Gruno *et al.*, 2004). The nonradioactive reduction can be easily achieved by using the treatment of cellulose with a strong reducing agent, such as sodium borohydride (Figure 4). Unfortunately, the reduction to alcohols lacks the required sensitivity of detection (Arai *et al.*, 1989). Although the [^{3}H]-label in the reducing end provides a high sensitivity of detection, it was shown relatively unstable (Gruno *et al.*, 2004). A plausible alternative for the reduction is the labeling of reducing ends on cellulose with fluorescent amines, such as anthranilic acid (AA) (Figure 4).

The reductive amination of reducing ends of sugars is a common practice in glycoconjugate chemistry (Anumula, 2006). In the first study employing the reducing end labeling of cellulose *via* reductive amination, the labeling with AA was performed in water (Kipper *et al.*, 2005). Pioneered by the studies of Anumula, buffered methanol was shown to be a superior environment in terms of reaction time and yields for reductive amination of sugars (Anumula, 1994, 2006). This prompted us to test the labeling of cellulose with AA in buffered methanol (Ref I). We made a thorough comparison of labeling of cellulose with

AA in three common solvents used for reductive amination: (i) water, (ii) DMSO, (iii) buffered methanol. The reactions were optimized also in terms of concentration of the reagents (cellulose, AA, $NaCNBH_3$) and reaction time (Ref I, Figure 1). The quantitative labeling with minimal incorporation of unspecific label was achieved in buffered methanol. Consequently, the optimal conditions for cellulose labeling were the following: in buffered methanol containing 50 mM AA, 0.5 M $NaCNBH_3$ and 2 mg/ml cellulose for 1h at 80 ^{o}C. The reaction conditions optimized for labeling of cellulose with AA (Ref I) were later shown to be optimal also for labeling of cellulose with 2,6-diaminopyridine (Kurašin & Väljamäe, 2011) and AA-labeling of chitin (Kurašin *et al.*, 2015). Most importantly, as first shown by Kurašin and Väljamäe (2011), and later here (Ref II), the fluorescence labeling of cellulose turned out to be valuable in determining the values of important kinetic parameters (P^{app} and k_{off}) of processive CBHs.

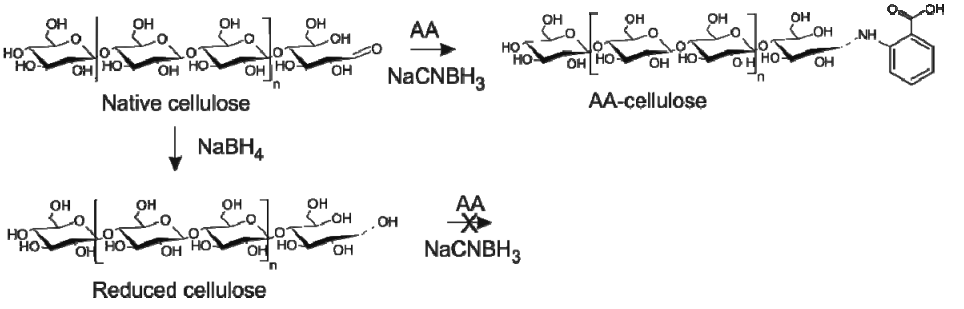

Figure 4. Reductive amination of cellulose reducing ends with AA. Using a mild reducing agent $NaCNBH_3$, aldehyde groups of cellulose are converted to corresponding aminoalditols. Compared to $NaCNBH_3$, $NaBH_4$ is a more powerful reducing agent and reduces aldehyde groups to alditols, which cannot react in reductive amination. Adapted from Kurašin and Väljamäe (2011).

AA-labeled cellulosic substrates were tested for their suitability to determine the mode of action of CBHs Cel7A and Cel6A. As first presented by Nutt *et al.* (1998), cellulases can be functionally classified by constructing the progress curves (released end-label *versus* total degradation) using the hydrolysis data of end-labeled cellulose. Though the hydrolysis of different AA-labeled celluloses by GH7 and GH6 CBHs were consistent with their expected mode of action, it appeared that not all AA-labeled substrates were equally suitable for determining the chain end preference. For example, the reducing ends of highly crystalline cellulose that are buried inside the crystal are hidden from the labeling and cause unequal distribution of the label. Since cellulose surface is the first target for cellulases, the unequal distribution of the label increases the initial slope of the progress curve. We found that the most suitable substrate for generating progress curves was AA-labeled regenerated amorphous Avicel, where the differences between the progress curves of GH7 and GH6 CBHs were most obvious (Ref I, Figure 3). The progress curve of *Tr*Cel7A was clearly convex and progressed above the 1:1 line. The 1:1 line indicates the hydrolysis

pattern where the extent of the released end-label equals to the extent of the total degradation. Therefore, the convex progress curve above the 1:1 line is characteristic to the enzymes with reducing-end preference (Nutt *et al.*, 1998). The progress curve of *Tr*Cel6A started below the 1:1 line and was shaped concavely, indicating the preference of the nonreducing end. The progress curves on AA-labeled regenerated amorphous Avicel were also generated for Cel7D and Cel6A from *Phanerochaete chrysosporium*, which are analogues of *Tr*Cel7A and *Tr*Cel6A, respectively. Progress curves of Cel7D and Cel6A from *Phanerochaete chrysosporium* overlapped with the ones of *Tr*Cel7A and *Tr*Cel6A, respectively (Ref I, Figure 3).

Taken together, using the AA-labeled substrate for the cellulose hydrolysis to generate progress curves is the rationale for the rapid assessment of the directionality of processive CBHs. However, interpretation of the progress curves is complicated by endo-mode initiations and processivity of enzymes, which both affect the shape of the curve (Nutt *et al.*, 1998). Our results also show that the substrate properties, such as the availability of reducing ends for the labeling, influence the extent of curving. Therefore, methods that are more precise should be used to confirm the knowledge acquired from progress curves.

AA-labeled cellulose can also be used in experiments to determine the probability of endo-mode initiations of reducing-end specific cellulases. The method is based on parallel quantification of total initiations (sum of exo- and endo-initiations) and only reducing end specific initiations (exo-initiations) on cellulose (Kurašin & Väljamäe, 2011). Performing the hydrolysis on fluorescence-labeled cellulose, the concentration of released end label represents the number of the reducing end specific initiations if the conditions are selected so that the probability of repeated attacks from the same chain is negligible. To reveal the number of total initiations on cellulose, the hydrolysis must be performed under the same conditions, but using the reduced cellulose as a substrate. In that case, the number of IRGs generated to reduced cellulose equals to the number of total initial attacks. The amount of endo-initiations can be found as a difference between the total number of initiations (exo + endo attacks) and the reducing end specific initiations (exo-attacks).

4.2. The role of Trp38 and CBM in the action of *Tr*Cel7A (Ref II)

Cellulase *Tr*Cel7A has a multimodular structure, consisting of CD and CBM that are connected through a glycosylated linker peptide (Figure 5A). The main role of CBM is to mediate the binding of the enzyme to cellulose (Carrard *et al.*, 2000; McLean *et al.*, 2002; Herve *et al.*, 2010). CBM largely facilitates the binding to crystalline substrates, and its presence increases the binding at low substrate concentrations significantly (Sugimoto *et al.*, 2012; Cruys-Bagger *et al.*, 2013b; Guo & Catchmark, 2013; Várnai *et al.*, 2013). The glycosylated linker

between the CD and CBM was also shown to enhance the binding of CBM (Payne *et al.*, 2013b). The catalysis is performed by CD and the parameters of catalysis (k_{cat} and P^{app} values) are unaffected by the presence of the CBM-linker (Igarashi *et al.*, 2009; Jalak *et al.*, 2012; Cruys-Bagger *et al.*, 2013b). The active site rests in CD and contains 10 subsites (–7 to +3) for binding of glucose residues in cellulose (Divne *et al.*, 1998). The subsites –7 to –1 are at the entering side from the catalytic site and are denoted as substrate binding subsites. In contrast, subsites +1 to +3 are for product binding. The active site of *Tr*Cel7A is lined with four conserved aromatic residues: Trp38, Trp40, Trp367 and Trp376, which form hydrophobic stacking interactions with glucose moieties of the substrate (Divne *et al.*, 1998) (Figure 5B). Trp38 and Trp40 locate at the substrate entrance region of the tunnel, at subsites –7 and –4, respectively. Trp367 and Trp376 edge the catalytic site and are suggested to participate in catalytic complex formation (Knott *et al.*, 2014a). The substitution of aromatic residues with non-aromatic ones has usually a negative impact on the activity and processivity of CBHs and chitinases (Zhang *et al.*, 2000; Horn *et al.*, 2006; Li *et al.*, 2007; Igarashi *et al.*, 2009; Zakariassen *et al.*, 2009; Payne *et al.*, 2011; Nakamura *et al.*, 2013; Kostylev *et al.*, 2014; Kurašin *et al.*, 2015). The substitution of Trp40 at the tunnel entrance of *Tr*Cel7A with alanine restricts the chain loading on a crystalline substrate (Igarashi *et al.*, 2009; Nakamura *et al.*, 2013). Also, the Trp38 substitution with alanine though restricting the enzyme-substrate complex formation, still has a positive effect on enzyme activity at saturating substrate loads (Kari *et al.*, 2014). Studying four different *Tr*Cel7A variants, WT, W38A and their truncated versions lacking the CBM-linker, WT_{CD} and $W38A_{CD}$, Kari and co-workers found that the V_{max} values of the variants increased in the following order: $W38A_{CD}$ > W38A > WT_{CD} > WT . We studied these enzyme variants in terms of feeding of cellulose chain, processive hydrolysis and enzyme dissociation to reveal any changes in kinetic parameters (k_{off}, P^{app}, k_{on}) that can be responsible for increased activity of *Tr*Cel7A W38A (Ref II).

Several studies have identified the dissociation as the rate limiting step in processive cellulose hydrolysis by *Tr*Cel7A (Kurašin & Väljamäe, 2011; Praestgaard *et al.*, 2011; Cruys-Bagger *et al.*, 2012a; Cruys-Bagger *et al.*, 2013b). The rapid rate retardation is proposed to be caused by the slow dissociation of the enzyme that has been stalled by steric obstacles (Jalak & Väljamäe, 2010; Igarashi *et al.*, 2011; Kurašin & Väljamäe, 2011). The exact nature of these obstacles is not known, but they can be associated with irregularities in cellulose structure (Kurašin & Väljamäe, 2011). According to the obstacle model, the steady state rate of *Tr*Cel7A on cellulose can be given as: $v_{CB}=k_{off}P^{app}[E]_{bound\text{-}OA}$ (Jalak & Väljamäe, 2010) whereas P^{app} is limited by the length of the obstacle-free path on cellulose (Kurašin & Väljamäe, 2011).

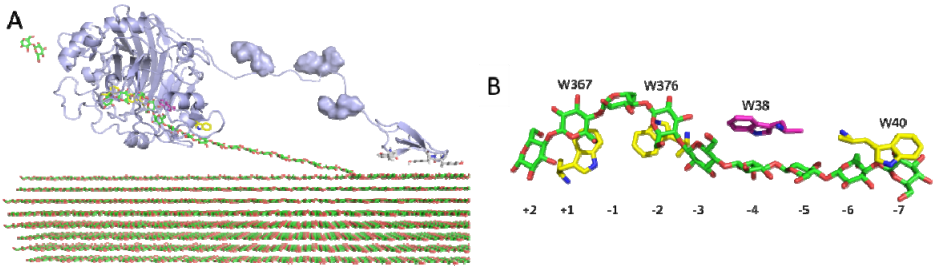

Figure 5. **Structure of *Tr*Cel7A.** A, A schematic representation of *Tr*Cel7A performing processive hydrolysis of cellulose. The enzyme is shown in blue and cellulose in green. *Tr*Cel7A has a two-domain structure, consisting of CD that is connected to CBM by the glycosylated linker peptide. The active site rests in CD and is occupied by the cellulose chain. The tunnel-shaped active site of *Tr*Cel7A is lined with four aromatic residues: Trp40, Trp376, Trp367 (yellow), and Trp38 (magenta). B, The aromatic residues in the active site of *Tr*Cel7A form hydrophobic stacking interactions with the glucose moieties. The numbers represent the binding subsites for the glucose moieties. Trp40 and Trp38 locate at the substrate binding subsites, Trp376 and Trp367 surround the catalytic centre of the active site. The figure is adapted from Ref II, Figure 1.

For finding P^{app}, the generation of IRGs on reduced cellulose was measured in parallel with measurements of the released SRGs (Kurašin & Väljamäe, 2011). P^{app} was found as the slope of the plot in coordinates $[RG]_{tot}$ *versus* [IRG], where $[RG]_{tot}=[IRG]+[SRG]$. The P^{app} values were measured on two different substrates, reduced bacterial cellulose (rBC) and reduced amorphous cellulose (rAC) (Ref II, Tables 1 and 2). The P^{app} values on rBC were higher than on rAC. One may speculate that BC contains less irregularities and serve longer obstacle-free paths for processive runs than more disordered AC (Kurašin & Väljamäe, 2011). With both substrates, the CBM-linker had only a moderate effect on processivity, whereas W38A mutation resulted in about twofold decrease in P^{app} value. Because of the low activity of $W38A_{CD}$ on a crystalline substrate, we could not measure the production of IRGs, and thus P^{app} of $W38A_{CD}$ on rBC remained unknown. P^{app} of all four variants could be measured on rAC. The P^{app} value of $W38A_{CD}$ on rAC was similar to that of W38A variant, suggesting that the W38A substitution is the primary cause of decreased P^{app} value compared to WT. Although the W38A substitution lowered the P^{app} value of the enzyme, the variants with this substitution showed higher rates of product release (measured in SRGs) than their WT counterparts on rAC (Ref II, Figure 4A).

This prompted us to determine if the increased off-rate is responsible for increased activity of the W38A variants. The off-rates were found by using two different approaches: (i) by measuring the rate constant of the formation of IRGs and (ii) by measuring the exchange rate of enzyme between the two substrates (SEE). First, the off-rates from Avicel were measured by using SEE (Ref II, Figure 2). The off-rates of the variants increased in the following order: $W38A > WT_{CD} > WT$ (Ref II, Table 1). Unfortunately, we could not measure

the off-rate of $W38A_{CD}$ using SEE. This could be due to rapid dissociation and/or inefficient binding of $W38A_{CD}$. Next, we determined the off-rates by measuring the production of IRGs on reduced cellulose. There was a good consistency between the k_{IRG} values measured on rBC and off-rates from SEE measured on Avicel (Ref II, Table 1). The k_{IRG} values were also measured on rAC (Ref II, Table 2). The k_{IRG} values on rAC were significantly higher than corresponding figures on crystalline substrates. Similarly to the results on crystalline substrate, the removal of CBM-linker and/or W38A substitution increased the k_{IRG} values on an amorphous substrate. The k_{IRG} values on rAC reveal a positive correlation between the activity (Ref II; Figure 4A) and the off-rates (Ref II; Table 2). Collectively, the results confirm that higher activity of both Trp38 variants of *Tr*Cel7A compared to their WT counterparts is due to their increased off-rates.

The W38A substitution had a moderately negative effect on binding of *Tr*Cel7A to cellulose (Kari *et al.*, 2014). We confirmed the weaker binding of Trp38 variants to rBC in comparison to WT by measuring $[E]_{bound\text{-}OA}$. The binding was weakest with $W38A_{CD}$. Because of too weak binding of the CDs, only the binding of the intact variants was studied further in more detail (Ref II; Figure 5). The binding of WT to BC was stronger than that of W38A at the levels of $E_{bound\text{-}tot}$ and $E_{bound\text{-}OA}$. The most remarkable difference between the binding of two variants was a significant population of $E_{bound\text{-}FA}$ of W38A.

The binding of the variants was more efficient on AC, due to the high binding capacity of this substrate. Therefore, it was a suitable substrate to measure the binding of all four variants (Ref II, Figure 6A). The differences at the level of $E_{bound\text{-}OA}$ between the variants is evident when comparing the half-saturating substrate concentrations (Ref II, Table 2). Although both, the absence of the CBM-linker and the Trp38 substitution decreased the binding of *Tr*Ce7A, the most prominent was a sharp decrease in binding caused by both modifications present. The half-saturating substrate concentrations ($S_{0.5}$) can be dissected into its on- and off-rate components, according to $k_{on}=k_{IRG}/S_{0.5}$. We found that inefficient binding of $W38A_{CD}$ was mainly caused by the decreased on-rate component (Ref II, Table 2). The closer look into the on-rate components revealed that the Trp38 mutation was largely compensated by the presence of the CBM-linker and vice versa. Contrarily, the off-rate of the enzyme was affected only by the W38A mutation and was independent of the presence of the CBM-linker. This moderate effect of either the CBM-linker or the W38A mutation to the off-rate in parallel with drastically decreased binding affinity of the $W38A_{CD}$ suggests that both, the Trp38 and the CBM-linker are important in the association of the enzyme with crystalline substrate. Since the active site binding that we measured, implies that the cellulose chain has progressed at least to the binding subsite –2, our results suggest that both, the CBM-linker and the Trp38 are needed for efficient feeding of the cellulose chain into the active site tunnel of *Tr*Cel7A. The role in feeding the cellulose chain has been previously demonstrated also for Trp40, locating at the edge of the tunnel entrance of *Tr*Cel7A (Igarashi *et al.*, 2009; Nakamura *et al.*, 2013). Computational studies

with the CD of W40A mutant demonstrated that after passing through the tunnel entrance region (up to subsite –5) the further sliding of the cellulose chain into the tunnel is not affected by the mutation (Nakamura *et al.*, 2013).

It is well known that the performance of the enzymes with different modes of action results in a synergistic and complete degradation of a polysaccharide. Therefore, we also assessed the effect of the Trp38 mutation to the performance of *Tr*Cel7A in synergistic hydrolysis of BC. Here, only the intact variants were studied. Low BC concentrations are optimal for the synergistic hydrolysis of BC by WT supplemented with EG and β-glucosidase (Jalak *et al.*, 2012). The activity of W38A in synergistic hydrolysis was very low at BC concentrations optimal for WT but increased with the increasing BC concentration (Ref II, Figure 7A). A low activity of W38A in a synergistic mixture can be associated with inefficient binding of the variant. Indeed, when measuring the binding of W38A at active site level, we found that, in contrast to WT (Jalak *et al.*, 2012), the binding of W38A was reduced in the presence of EG (Ref II, Figure S1). Furthermore, at BC concentrations below 0.5 g/l (optimal for WT) the active site mediated binding of W38A remained below the detection limits. We also found that, while stimulating the activity of WT, the pretreatment of BC with EG had a little or even negative effect on the activity of W38A (Ref II, Figure 7B). The decreased binding efficiency in the presence of EG and the poor performance on EG-treated cellulose suggest that EG may have a negative effect on substrate accessibility by W38A. One may speculate that the original loose chain-ends of BC are trimmed shorter by the action of EG and the remaining blunt chain-ends are more difficult to feed into the active site tunnel of W38A.

To conclude, the main role of Trp38 in the active site of *Tr*Cel7A is feeding the cellulose chain into the active site tunnel. Trp38 contributes also to enzyme processivity by reduction of the off-rate of the enzyme. The decreased binding strength at the entrance region of the active site may result in an increased activity against cellulose at the conditions where the availability of chain ends compensates the deficiency in feeding. However, the concomitant feeding deficiency is even more outstanding in synergistic cellulose hydrolysis. This implies that in cooperative action with EGs, the inter-domain synergism between the CBM-linker and the CD is a pre-requisite for efficient hydrolysis of cellulose.

4.3. Anomeric selectivity and product profile of *Tr*Cel7A (Ref III)

*Tr*Cel7A performs cellulose hydrolysis processively and after every catalytic act advances one cellobiose unit further, liberating cellobiose$_\beta$ as the main product (Divne *et al.*, 1994; Divne *et al.*, 1998; Medve *et al.*, 1998; von Ossowski *et al.*, 2003; Fox *et al.*, 2012; Knott *et al.*, 2014b). Yet, production of a small amount of odd-numbered products glucose and cellotriose has been also reported (Medve *et al.*, 1998; von Ossowski *et al.*, 2003). Although the origin of odd-numbered products is still an open question, processivity of the enzyme on

cellulose has been evaluated according to the different combinations of odd- and even-numbered products produced by the enzyme (Medve *et al.*, 1998; von Ossowski *et al.*, 2003; Vuong & Wilson, 2009; Kern *et al.*, 2013; Hamre *et al.*, 2014; Kari *et al.*, 2014; Kostylev *et al.*, 2014). Such approach is attractive because the product profile of the enzyme can be determined by using simple chromatographic measurements.

Mostly it is assumed that the odd-numbered products are formed upon the initial cut, whereas cellobiose is formed upon following processive cuts (Horn *et al.*, 2012). The formation of odd-numbered products upon first cut is often explained by different initial binding modes of *Tr*Cel7A with a cellulose chain that, in turn, is determined by structural properties of the substrate (Nidetzky *et al.*, 1994; Barr *et al.*, 1996; Medve *et al.*, 1998; Teeri *et al.*, 1998; von Ossowski *et al.*, 2003; Fox *et al.*, 2012; Hamre *et al.*, 2014; Kostylev *et al.*, 2014). In cellulose chain, glucose residues are rotated 180 degrees relative to one another and, therefore, the glycosidic bonds have a zigzag appearance (Figure 6). As interactions between the active site residues of the enzyme and glucose moieties of the entering cellulose chain hinder flipping of the entering chain, two mirrored orientations of the entering chain can be considered and are denoted here as A- and B-chain. Furthermore, both orientations of cellulose chain can be in two different configurations depending on the anomeric configuration of the reducing end (Figure 6). When the A-chain enters the tunnel so that the product subsites (+1, +2) are filled, the glycosidic bond is in scissile position. With this binding mode, the initial-cut product is cellobiose. Contrarily, when the B-chain enters the tunnel, the first and also the third bond are productively orientated for the hydrolysis and during the catalysis the product-binding subsites, either (+1) or (+1, +2, +3), are filled (Figure 6). The initial-cut products in this case are either glucose or cellotriose. Assuming no preference in the acquisition of A- and B-chains by *Tr*Cel7A, the probability for picking up either of them is equal. If so, the odd-numbered and even-numbered initial-cut products should be released in equal amounts.

We analysed the initial-cut product pattern of *Tr*Cel7A on soluble oligosaccharides and found that the prevalent initial-cut product of *Tr*Cel7A was odd-numbered. This finding is in accordance with the earlier reports (Vrsanska & Biely, 1992; Nidetzky *et al.*, 1994; Barr *et al.*, 1996). The product profiles of *Tr*Cel7A from the hydrolysis of cellooligosaccharides of different lengths (DP 4–6) are listed in Ref III, Table 1. Product profiles were further used to calculate probability of odd-numbered initial-cut product (P_{odd}) on each oligosaccharide. For calculating P_{odd} for celloheptaose and cellooctaose, the previously published data (Nidetzky *et al.*, 1994) were used. Detailed description of finding P_{odd} are given in supplementary material of Ref III. P_{odd} increased with the increasing DP of the substrate and levelled off around 0.80 for longer cellooligosaccharides (Ref III, Table 1).

The product profile of *Tr*Cel7A was also characterized on Avicel using ^{18}O-labeling technique (carried out by Dr. Jeppe Kari, Roskilde University, Denmark). Performing enzymatic hydrolysis in $H_2{}^{18}O$, the ^{18}O label is incorporated only to

the products of processive hydrolysis, but not to the initial-cut products (Ref III, Figure 2). To complete the catalytic reaction, nucleophilic water attacks the glycosyl-enzyme intermediate and ^{18}O-labeled hydroxyl is incorporated into the reducing end of the shortening cellulose chain. During the next cleavage by *Tr*Cel7A the ^{18}O-labeled product is released. Therefore, all products, except the initial-cut one, carry the ^{18}O-label and one can distinguish between the initial- and processive-cut products. The concentrations of unlabeled and labeled products are given in Ref III, Table 2. The main unlabeled product and, hence, the major initial-cut product at Avicel hydrolysis in $H_2{}^{18}O$ was glucose (79%), followed by cellobiose (17%) and cellotriose (4%). The prevailing labeled product and, hence, the main processive-cut product was cellobiose (94%). Labeled glucose and cellotriose were also detected, but in small amounts. Interestingly, while most of the released glucose (81% of the total) was unlabeled and therefore released upon the initial cut, 86% of total released cellotriose was labeled. The origin of the labeled odd-numbered products cannot be assessed on the basis of the current data. One may suggest that these labeled odd-numbered products may result (i) from initial attacks from the nonreducing ends, (ii) as the final products of fully hydrolysed cellulose chains, (iii) as the products of tranglycosylation or (iv) from the secondary hydrolysis of cello-tetraose. The important finding here was that P_{odd} of cellulose hydrolysis was close to the P_{odd} of longer cellooligosaccharides. We recognize that this result does not support the previously suggested simple mechanism of liberating even- and odd-numbered initial-cut products in equal amounts. Considering that the molecular dynamics simulations have shown that cellulose chain orientation (A-*versus* B-chain) does not affect its entering to enzyme's active site (Ghattyvenkatakrishna *et al.*, 2013), the dominance of odd-numbered initial-cut products is unlikely the result of selective threading of the cellulose chain at the tunnel entrance. Hence, seeking the mechanism behind the dominance of odd-numbered initial-cut products, we further focused on binding at product-binding subsites of the enzyme.

The specific hydrogen bonding interactions in product-binding subsites (+1,+2) are the driving force of processive movement of the cellulase. Moreover, they are responsible for strong cellobiose inhibition of *Tr*Cel7A (Divne *et al.*, 1998; von Ossowski *et al.*, 2003; Andric *et al.*, 2010a; Teugjas & Väljamäe, 2013; Knott *et al.*, 2014a). We found that the strength of cellobiose inhibition depends on anomeric configuration of the reducing end of cellobiose. Inhibition experiments with cellobiose either in cellobiose$_\beta$ or cellobiose$_\alpha$ anomeric form showed that β-anomer of cellobiose exerted stronger inhibition. The strength of the inhibition decreased with aging of the cellobiose$_\beta$ preparation. The opposite was true for experiments conducted with cellobiose$_\alpha$ (Ref III, Figure 4A). In both cases, the inhibition strength changed with the age of cellobiose preparation according to the rate of mutarotation of cellobiose measured under comparable conditions (Cruys-Bagger *et al.*, 2012b). Measurements of anomer-specific inhibition of endoglucanase *Tr*Cel7B revealed no anomeric selectivity (Ref III, Figure 4B).

The most likely candidate to interact with the reducing end of cellobiose in +2 subsite of *Tr*Cel7A is Arg394. This residue forms a hydrogen bond with the anomeric hydroxyl group in the reducing end of cellulose (Stahlberg *et al.*, 1996; Divne *et al.*, 1998) (Ref III, Figure 6). *Tr*Cel7B has an alanine in the corresponding position, and the binding efficiency with the product at +2 subsite is considerably decreased compared to *Tr*Cel7A. Importantly, the insertion of arginine into the corresponding position in *Tr*Cel7B increases the binding efficiency at product-binding subsites and also the processive ability of the enzyme (Wang *et al.*, 2016). Thus, the arginine to alanine substitution in *Tr*Cel7B is probably responsible for a decreased binding affinity of the subsite +2. Based on current data we could not verify that this specific interaction is the cause of the anomeric selectivity of *Tr*Cel7A in +2 binding site, but if this speculation is true, the high processivity of *Tr*Cel7A may at least partially result from anomer-specific interaction in the binding subsite +2.

Returning to the mechanistic interpretation of the prevalence of odd-numbered initial-cut products, we suggest that it can be probably linked to anomeric selectivity in +2 binding subsite. Considering that the hydroxyl group in the reducing end can be either in α- or β-configuration, we have 4 possible chain forms (A-chain$_\alpha$, A-chain$_\beta$, B-chain$_\alpha$ and B-chain$_\beta$) (Figure 6). Mutarotation between the α- and β-configurations is possible, but the rate is slower than the catalytic turnover of *Tr*Cel7A. From four chain types, only an A-chain$_\beta$ creates a regular complex that is formed also during processive cellulose hydrolysis with cellobiose$_\beta$ as the initial-cut product (Figure 6).

It is more difficult to interpret the possible initial-cut products in the case A-chain$_\alpha$ enters the active site. When the reducing end is in α-configuration, the anomeric selectivity in +2 product-binding subsite will lead to the formation of a less stable enzyme-substrate complex. Alternatively, the chain may slide two subsites further and produce a more stable complex with the enzyme. In that case, the initial-cut product will be cellotetraose. Either possibility is not supported by the measured concentrations of the hydrolysis products of *Tr*Cel7A on Avicel. A low concentration of cellotetraose (Ref III, Figure 1, upper panel) and cellobiose from the initial cut (Ref III, Table 2) indicates that the A-chain$_\alpha$ is probably a poor substrate for *Tr*Cel7A forming mainly a nonproductive complex with the enzyme.

In the case of binding of the B-chain, the glycosidic bond is in scissile position when the reducing end enters either the subsite +1 or +3 (Figure 6). In both cases the initial-cut product is odd-numbered, glucose or cellotriose, respectively. The configuration of the reducing end of the product depends on the configuration of the chain end, glucose$_\alpha$ or cellotriose$_\alpha$ for the B-chain$_\alpha$, and glucose$_\beta$ or cellotriose$_\beta$ for the B-chain$_\beta$. The experimental results indicate that cellotriose is released as the initial-cut product in very low quantities and the main odd-numbered initial-cut product is glucose. Therefore, the first scenario, whereby the reducing group of the B-chain binds initially in subsite +1, is more likely.

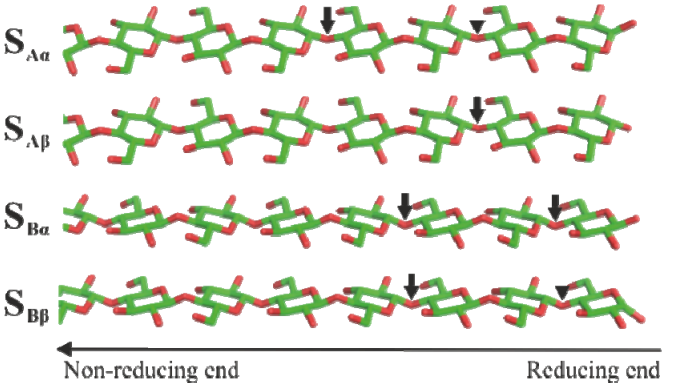

Figure 6. Four different forms of a cellulose chain that may enter the active site of *Tr*Cel7A. Both types of arrows (▼,↓) indicate the scissile bonds that are in correct orientation for the initial cleavage. The arrows with the tail (↓) show the positions where the reducing end of the chain is also in a correct anomeric configuration (β in +2 and α in +1) in the productive complex with the enzyme. The scheme is modified from Ref III, Figure 7D.

Taken together, the considered possibilities of initial complex formation between *Tr*Cel7A and cellulose chain explain at least partly the dominance of initial-cut glucose. In addition, we suggest that the anomeric selectivity in the binding subsite +2 may be linked to high processive potential of the enzyme. Anomeric selectivity in active sites of GHs has been reported before, for example for chitinases (Aronson *et al.*, 2003; Chou *et al.*, 2006; Honda *et al.*, 2008; Fukamizo *et al.*, 2009; Suginta *et al.*, 2009; Eide *et al.*, 2013). There are also few studies denoting a link between anomeric selectivity and enzyme processivity. In contrast to our hypothesis about its necessity for the processive movement of *Tr*Cel7A, there are few cases where the anomeric selectivity in product-binding subsite opposes to the processive movement of the enzyme (Honda & Kitaoka, 2004; Fushinobu *et al.*, 2005; Aronson & Halloran, 2006). For example, the enzymes chitobiase (Aronson & Halloran, 2006) and exo-oligoxylanase (Honda & Kitaoka, 2004; Fushinobu *et al.*, 2005) release a monomeric product. Using a retaining mechanism, both enzymes produce a new reducing end at the subsite –1 with the opposite anomeric configuration to that preferred at the subsite +1, and thereby disabling the processive movement of the enzyme.

CONCLUSIONS

Enzymatic cellulose degradation is a complex process involving multi-modular enzymes and an insoluble recalcitrant substrate. Our findings contribute to the molecular-level understanding of enzymatic conversion of cellulose. In biochemical studies, the molecular aspects of cellulase action on cellulose are conventionally addressed by using either of the two approaches: (i) modification of the enzyme or (ii) altering the substrate (*e.g.* through labeling). Here, we used both these approaches separately and also in combination with each other to characterize the performance of *Tr*Cel7A on cellulose. The most important conclusions of this study are listed below.

1. The fluorescence labeling with anthranilic acid in buffered methanol is an efficient and selective method to label the reducing ends of cellulose chains. As the reducing end specific fluorescence labeling enables sensitive detection of reducing ends, it is a valuable tool to measure the mode of action, endo-probability, processivity and dissociation rate constant of reducing-end specific cellulases.

2. The primary role of Trp38 near the entrance of the active site of *Tr*Cel7A is feeding of cellulose chain into the active site tunnel. Beside this particular role of Trp38, a synergistic effect of it with CBM-linker in feeding was shown. Trp38 was also confirmed as an important determinant of processivity of *Tr*Cel7A *via* reducing the off-rate.

3. The predominant initial-cut product of the hydrolysis of both, cellooligosaccharides and insoluble cellulose by *Tr*Cel7A was glucose. This phenomenon can at least partly be due to selectivity for β-anomer in the product-binding subsite +2. Our results also suggest a possible link between anomer-selectivity in product-binding subsites and the processivity of the cellulase.

SUMMARY IN ESTONIAN

Tselluloosiahela sidumine protsessiivse tsellobiohüdrolaasi poolt

Üheks alternatiivseks tooraineks mootorikütuste aga ka kemikaalide tootmisel on taimne biomass. Taimse biomassi peamiseks polümeerseks komponendiks on tselluloos. Tselluloosi polümeer koosneb β-1,4-glükosiidse sideme kaudu ühendatud glükoosijääkidest. Tänu tselluloosi suurele hulgale taimedes ja selle komponentide (glükoosi) fermenteeritavusele, on tselluloos peamine biomassi komponent, millest toota bioetanooli. Kuna kääritajad mikroorganismid suudavad enamasti omastada mitte tselluloosi, vaid glükoosi, tuleb glükoosi molekule ühendav ahelstruktuur esmalt lagundada. Seda on optimaalseim teha ensümaatiliselt, kasutades loodusest isoleeritud organismide tselluloosi lagundavaid ensüüme – tsellulaase. Biomassi baasil toodetav bioetanool ei konkureeri siiski veel hinna poolest turul olevate fossiilsete mootorikütustega. Peamine pidev kuluallikas bioetanooli tootmisel on tsellulaaside suures mahus tootmine. Vajaminevat ensüümide hulka oleks võimalik vähendada, tootes ensümaatiliselt efektiivsemaid ensüüme. See omakorda eeldab aga detailset tsellulaaside molekulaarsete mehhanismide tundmist, et parendada tsellulaase teadmistepõhise insenergeneetilise modifitseerimise teel.

Tselluloosi ensümaatiline hüdrolüüs on kompleksne protsess. Ühelt poolt osaleb selles vees lahustumatu, enamjaolt kristallilise ehitusega substraat tselluloos, ja teiselt poolt hulk erineva toimemehhanismiga ensüüme – tsellulaase. Tsellulaaside struktuuri ja funktsiooni vaheliste seoste mõistmiseks on kasulik uurida erinevaid ensüüme isoleeritult. Tsellulaaside uurimiseks kasutatakse erinevaid tselluloosi mudelsubstraate, mille koostis on, erinevalt looduslikust tselluloosist, defineeritud ning mis võimaldab viia ensüümiuuringud läbi korratavates tingimustes.

Oma doktoritöös keskendusin peamiselt *Trichoderma reesei* tsellulaasi Cel7A uurimisele. Pehmemädanikseen *T. reesei* on kujunenud tänu kõrgele tsellulaaside produktsioonile mudelorganismiks tsellulolüütilise süsteemi uurimisel. Kõige suuremal hulgal toodavad tselluloosi lagundavad mikroorganismid protsessiivseid tsellobiohüdrolaase, mis viivad ühe tselluloosile seostumise kohta läbi mitu järjestikust katalüüsiakti. Peamine *T. reesei* sekreteeritav protsessiivne tsellobiohüdrolaas on Cel7A, mis moodustab organismi poolt eritatavate valkude koguhulgast ligikaudu 60%. *TrCel7A* on kahedomeense ehitusega. Esmast tselluloosile seondumist vahendav seondumise domeen on seotud peptiidse linkeri kaudu katalüütilise domeeniga. Glükoosijääkidest koosneval tselluloosiahelal eristatakse kahte keemiliselt erinevat otsa: redutseerivat ja mitteredutseerivat. *Tr*Cel7A alustab tselluloosi hüdrolüüsi ahela redutseerivast otsast.

Minu töö esimeseks eesmärgiks oli optimeerida tselluloosi redutseeriva otsa spetsiifilist fluorestsentsmärgistamist ning uurida fluorestsentsmärgistatud substraadi sobivust tsellulaaside otsaeelistuse määramiseks (Ref I). Katsetulemused näitasid, et tselluloosi märgistamine reduktiivse amineerimise teel fluorestseeruva amiini antraniilhappega toimub kõige efektiivsemalt puhverdatud

metanoolis. Märgistamine toimus redutseeriva otsa spetsiifiliselt ja fluorestsentsmärke mõõtetundlikkus oli piisav, et määrata ensüümi poolt vabastatava otsmärgise hulka. Tselluloosi fluorestsentsmärgistamine on nüüdseks kujunenud tähtsaks osaks protsessiivsete tsellobiohüdrolaaside kineetiliste parameetrite määramise metoodikas. Lisaks on fluorestsentsmärgistamist käesoleva töö raames optimeeritud tingimustel rakendatud ka kitiinil – nii kitinaaside otsaeelistuse kui ka kineetiliste parameetrite määramisel.

Töö teine eesmärk oli välja selgitada aromaatse aminohappe Trp38 roll *Tr*Cel7A aktiivtsentris (Ref II). Ensüümi *Tr*Cel7A aktiivtsentris on lagundatava tselluloosiahela glükoosijääkidega seondumiseks kümme seondumiskohta: –7 kuni –1 ja +1 kuni +3. Katalüütiline tsenter, kus toimub glükosiidsideme hüdrolüüs, asub seondumiskohtade –1 ja +1 vahel. Tselluloosiahel siseneb *Tr*Cel7A tunnelikujulisse aktiivtsentrisse, redutseeriv ots ees seondumiskoha –7 suunalt ning seondub üle aktiivtsentri. Tsellulaasidele on omane aromaatsete aminohappejääkide esinemine aktiivtsentris. Ensüümil *Tr*Cel7A toimub kümnest glükoosijäägi seondumiskohast neljas seondumine aromaatsete aminohappejääkide kaudu. Üks neist on Trp38, mis asub aktiivtsentri tselluloosiahela sissepääsu lähedal – seondumiskohas –4. Kasutades mutantset *Tr*Cel7A ensüümi, kus Trp38 oli asendatud alaniiniga, uurisime Trp38 rolli aktiivtsentris. Leidsime, et Trp38 on oluline ensüümi protsessiivsuses. Mutantne ensüüm dissotsieerus tselluloosilt kiiremini, mistõttu oli ka selle protsessiivsus väiksem. Kõige enam mõjutas Trp38Ala mutatsioon tselluloosiahela seondumist ensüümi aktiivtsentrisse. Lisaks kirjeldasime seostumisdomeeni ja Trp38 vahelist sünergismi tselluloosiahela seondumisel aktiivtsentrisse.

Doktoritöö kolmas eesmärk oli välja selgitada *Tr*Cel7A paarituarvuliste produktide tekke mehhanism. Kuna tselluloosiahelas kõrvuti asetsevad glükoosijäägid on omavahel 180 kraadi pööratud, siis on iga teine glükosiidside ahelas hüdrolüüsiks korrektse orientatsiooniga, mistõttu on valdav *Tr*Cel7A poolt vabastatav produkt dimeerne üksus tsellobioos. Siiski vabastab ensüüm väiksemas koguses ka paarituarvulisi produkte – glükoosi ja tsellotrioosi. Leidsime, et valdavalt vabaneb glükoos *Tr*Cel7A esimese lõike produktina, samas kui peamine protsessiivse katalüüsi produkt on tsellobioos. Uurides seda fenomeni põhjustavaid molekulaarseid mehhanisme leidsime, et *Tr*Cel7A produkti seondumiskohas +2 toimub anomeeri-spetsiifline glükoosijäägi seondumine, mistõttu saab sinna seonduda β-konfiguratsiooniga glükoosijääk. Kui tselluloosiahel ei ole redutseerivas otsas β-konfiguratsiooniga, suunab ensüüm arvatavasti ahelaotsa +1 (või +3) seondumiskohta ja esimese lõike produktina vabastataksegi glükoos (või tsellotrioos). Pakume välja hüpoteesi, et β-anomeeri eelistatud seondumine +2 seondumiskohta on oluline ka ensüümi protsessiivsuse tagamisel.

REFERENCES

Andric, P., Meyer, A. S., Jensen, P. A., & Dam-Johansen, K. (2010a). Reactor design for minimizing product inhibition during enzymatic lignocellulose hydrolysis: I. Significance and mechanism of cellobiose and glucose inhibition on cellulolytic enzymes. *Biotechnol Adv, 28*(3), 308–324.

Andric, P., Meyer, A. S., Jensen, P. A., & Dam-Johansen, K. (2010b). Reactor design for minimizing product inhibition during enzymatic lignocellulose hydrolysis: II. Quantification of inhibition and suitability of membrane reactors. *Biotechnol Adv, 28*(3), 407–425.

Anumula, K. R. (1994). Quantitative determination of monosaccharides in glycoproteins by high-performance liquid chromatography with highly sensitive fluorescence detection. *Anal Biochem, 220*(2), 275–283.

Anumula, K. R. (2006). Advances in fluorescence derivatization methods for high-performance liquid chromatographic analysis of glycoprotein carbohydrates. *Anal Biochem, 350*(1), 1–23.

Arai, M., Sakamoto, R., & Murao, S. (1989). Different action of two avicelases from *Aspergillus aculateus*. *Agric Biol Chem*(5), 1411–1412.

Aronson, N. N., & Halloran, B. A. (2006). Optimum substrate size and specific anomer requirements for the reducing-end glycoside hydrolase di-N-acetylchitobiase. *Biosci Biotechnol Biochem, 70*(6), 1537–1541.

Aronson, N. N. Jr., Halloran, B. A., Alexyev, M. F., Amable, L., Madura, J. D., Pasupulati, L., . . . Van Roey, P. (2003). Family 18 chitinase-oligosaccharide substrate interaction: subsite preference and anomer selectivity of Serratia marcescens chitinase A. *Biochem J, 376*(Pt 1), 87–95.

Badino, S. F., Christensen, S. J., Kari, J., Windahl, M. S., Hvidt, S., Borch, K., & Westh, P. (2017). Exo-exo synergy between Cel6A and Cel7A from Hypocrea jecorina: Role of carbohydrate binding module and the endo-lytic character of the enzymes. *Biotechnol Bioeng*.

Barr, B. K., Hsieh, Y. L., Ganem, B., & Wilson, D. B. (1996). Identification of two functionally different classes of exocellulases. *Biochemistry, 35*(2), 586–592.

Baumann, M. J., Borch, K., & Westh, P. (2011). Xylan oligosaccharides and cellobiohydrolase I (TrCel7A) interaction and effect on activity. *Biotechnol Biofuels, 4*(1), 45.

Beckham, G. T., Bomble, Y. J., Matthews, J. F., Taylor, C. B., Resch, M. G., Yarbrough, J. M., . . . Crowley, M. F. (2010). The O-glycosylated linker from the Trichoderma reesei Family 7 cellulase is a flexible, disordered protein. *Biophys J, 99*(11), 3773–3781.

Beguin, P. (1990). Molecular biology of cellulose degradation. *Annu Rev Microbiol, 44*, 219–248.

Beguin, P., & Lemaire, M. (1996). The cellulosome: an exocellular, multiprotein complex specialized in cellulose degradation. *Crit Rev Biochem Mol Biol, 31*(3), 201–236.

Bezerra, R. M., Dias, A. A., Fraga, I., & Pereira, A. N. (2011). Cellulose hydrolysis by cellobiohydrolase Cel7A shows mixed hyperbolic product inhibition. *Appl Biochem Biotechnol, 165*(1), 178–189.

Bhat, K. M., Hay, A. J., Claeyssens, M., & Wood, T. M. (1990). Study of the mode of action and site-specificity of the endo-(1,4)-beta-D-glucanases of the fungus Penicillium pinophilum with normal, 1-3H-labelled, reduced and chromogenic cello-oligosaccharides. *Biochem J, 266*(2), 371–378.

Boisset, C., Fraschini, C., Schulein, M., Henrissat, B., & Chanzy, H. (2000). Imaging the enzymatic digestion of bacterial cellulose ribbons reveals the endo character of the cellobiohydrolase Cel6A from Humicola insolens and its mode of synergy with cellobiohydrolase Cel7A. *Appl Environ Microbiol, 66*(4), 1444–1452.

Boraston, A. B., Bolam, D. N., Gilbert, H. J., & Davies, G. J. (2004). Carbohydrate-binding modules: fine-tuning polysaccharide recognition. *Biochem J, 382*(Pt 3), 769–781.

Bu, L., Beckham, G. T., Shirts, M. R., Nimlos, M. R., Adney, W. S., Himmel, M. E., & Crowley, M. F. (2011). Probing carbohydrate product expulsion from a processive cellulase with multiple absolute binding free energy methods. *J Biol Chem, 286*(20), 18161–18169.

Bu, L., Nimlos, M. R., Shirts, M. R., Stahlberg, J., Himmel, M. E., Crowley, M. F., & Beckham, G. T. (2012). Product binding varies dramatically between processive and nonprocessive cellulase enzymes. *J Biol Chem, 287*(29), 24807–24813.

Carrard, G., Koivula, A., Soderlund, H., & Beguin, P. (2000). Cellulose-binding domains promote hydrolysis of different sites on crystalline cellulose. *Proc Natl Acad Sci U S A, 97*(19), 10342–10347.

Chanzy, H., & Henrissat, B. Unidirectional degradation of *Valonia* cellulose micro-crystals subjected to cellulase action *FEBS Letters, 184*(2), 285–288.

Chou, Y. T., Yao, S., Czerwinski, R., Fleming, M., Krykbaev, R., Xuan, D., . . . Huang, X. (2006). Kinetic characterization of recombinant human acidic mammalian chitinase. *Biochemistry, 45*(14), 4444–4454.

Claeyssens, M., Tomme, P., Brewer, C. F., & Hehre, E. J. (1990). Stereochemical course of hydrolysis and hydration reactions catalysed by cellobiohydrolases I and II from Trichoderma reesei. *FEBS Lett, 263*(1), 89–92.

Claeyssens, M., Van Tilbeurgh, H., Tomme, P., Wood, T. M., & McRae, S. I. (1989). Fungal cellulase systems. Comparison of the specificities of the cellobiohydrolases isolated from Penicillium pinophilum and Trichoderma reesei. *Biochem J, 261*(3), 819–825.

Cruys-Bagger, N., Alasepp, K., Andersen, M., Ottesen, J., Borch, K., & Westh, P. (2016). Rate of Threading a Cellulose Chain into the Binding Tunnel of a Cellulase. *J Phys Chem B, 120*(25), 5591–5600.

Cruys-Bagger, N., Elmerdahl, J., Praestgaard, E., Borch, K., & Westh, P. (2013a). A steady-state theory for processive cellulases. *FEBS J, 280*(16), 3952–3961.

Cruys-Bagger, N., Elmerdahl, J., Praestgaard, E., Tatsumi, H., Spodsberg, N., Borch, K., & Westh, P. (2012a). Pre-steady-state kinetics for hydrolysis of insoluble cellulose by cellobiohydrolase Cel7A. *J Biol Chem, 287*(22), 18451–18458.

Cruys-Bagger, N., Ren, G., Tatsumi, H., Baumann, M. J., Spodsberg, N., Andersen, H. D., . . . Westh, P. (2012b). An amperometric enzyme biosensor for real-time measurements of cellobiohydrolase activity on insoluble cellulose. *Biotechnol Bioeng, 109*(12), 3199–3204.

Cruys-Bagger, N., Tatsumi, H., Ren, G. R., Borch, K., & Westh, P. (2013b). Transient kinetics and rate-limiting steps for the processive cellobiohydrolase Cel7A: effects of substrate structure and carbohydrate binding domain. *Biochemistry, 52*(49), 8938–8948.

Davies, G. J., Mackenzie, L., Varrot, A., Dauter, M., Brzozowski, A. M., Schulein, M., & Withers, S. G. (1998). Snapshots along an enzymatic reaction coordinate: analysis of a retaining beta-glycoside hydrolase. *Biochemistry, 37*(34), 11707–11713.

Davies, G. J., Wilson, K. S., & Henrissat, B. (1997). Nomenclature for sugar-binding subsites in glycosyl hydrolases. *Biochem J, 321 (Pt 2)*, 557–559.

Din, N., Damude, H. G., Gilkes, N. R., Miller, R. C., Jr., Warren, R. A., & Kilburn, D. G. (1994). C1-Cx revisited: intramolecular synergism in a cellulase. *Proc Natl Acad Sci U S A, 91*(24), 11383–11387.

Divne, C., Stahlberg, J., Reinikainen, T., Ruohonen, L., Pettersson, G., Knowles, J. K., . . . Jones, T. A. (1994). The three-dimensional crystal structure of the catalytic core of cellobiohydrolase I from Trichoderma reesei. *Science, 265*(5171), 524–528.

Divne, C., Stahlberg, J., Teeri, T. T., & Jones, T. A. (1998). High-resolution crystal structures reveal how a cellulose chain is bound in the 50 A long tunnel of cellobiohydrolase I from Trichoderma reesei. *J Mol Biol, 275*(2), 309–325.

Doherty, W. O. S., Mousavioun, P., & Fellows, C. M. (2011). Value-adding to cellulosic ethanol: Lignin polymers. *Industrial Crops and Products, 33*(2), 259–276.

Eide, K. B., Lindbom, A. R., Eijsink, V. G., Norberg, A. L., & Sorlie, M. (2013). Analysis of productive binding modes in the human chitotriosidase. *FEBS Lett, 587*(21), 3508–3513.

Eriksson, T., Karlsson, J., & Tjerneld, F. (2002). A model explaining declining rate in hydrolysis of lignocellulose substrates with cellobiohydrolase I (cel7A) and endoglucanase I (cel7B) of Trichoderma reesei. *Appl Biochem Biotechnol, 101*(1), 41–60.

Foreman, P. K., Brown, D., Dankmeyer, L., Dean, R., Diener, S., Dunn-Coleman, N. S., . . . Ward, M. (2003). Transcriptional regulation of biomass-degrading enzymes in the filamentous fungus Trichoderma reesei. *J Biol Chem, 278*(34), 31988–31997.

Fox, J. M., Levine, S. E., Clark, D. S., & Blanch, H. W. (2012). Initial- and processive-cut products reveal cellobiohydrolase rate limitations and the role of companion enzymes. *Biochemistry, 51*(1), 442–452.

Fukamizo, T., Miyake, R., Tamura, A., Ohnuma, T., Skriver, K., Pursiainen, N. V., & Juffer, A. H. (2009). A flexible loop controlling the enzymatic activity and specificity in a glycosyl hydrolase family 19 endochitinase from barley seeds (Hordeum vulgare L.). *Biochim Biophys Acta, 1794*(8), 1159–1167.

Fushinobu, S., Hidaka, M., Honda, Y., Wakagi, T., Shoun, H., & Kitaoka, M. (2005). Structural basis for the specificity of the reducing end xylose-releasing exo-oligoxylanase from Bacillus halodurans C-125. *J Biol Chem, 280*(17), 17180–17186.

Gardner, K. H., & Blackwell, J. (1974). The hydrogen bonding in native cellulose. *Biochim Biophys Acta, 343*(1), 232–237.

Ghattyvenkatakrishna, P. K., Alekozai, E. M., Beckham, G. T., Schulz, R., Crowley, M. F., Uberbacher, E. C., & Cheng, X. (2013). Initial recognition of a cellodextrin chain in the cellulose-binding tunnel may affect cellobiohydrolase directional specificity. *Biophys J, 104*(4), 904–912.

Gruno, M., Väljamäe, P., Pettersson, G., & Johansson, G. (2004). Inhibition of the Trichoderma reesei cellulases by cellobiose is strongly dependent on the nature of the substrate. *Biotechnol Bioeng, 86*(5), 503–511.

Guerriero, G., Fugelstad, J., & Bulone, V. (2010). What do we really know about cellulose biosynthesis in higher plants? *J Integr Plant Biol, 52*(2), 161–175.

Guo, J., & Catchmark, J. M. (2013). Binding specificity and thermodynamics of cellulose-binding modules from Trichoderma reesei Cel7A and Cel6A. *Biomacromolecules, 14*(5), 1268–1277.

Habibi, Y., Lucia, L. A., & Rojas, O. J. (2010). Cellulose nanocrystals: chemistry, self-assembly, and applications. *Chem Rev, 110*(6), 3479–3500.

Hakansson, U., Fagerstam, L., Pettersson, G., & Andersson, L. (1978). Purification and characterization of a low molecular weight 1,4-beta-glucan glucanohydrolase from the cellulolytic fungus Trichoderma viride QM 9414. *Biochim Biophys Acta, 524*(2), 385–392.

Hallac, B.B., & Ragauskas, A.J. (2011). Analyzing cellulose degree of polymerization and its relevancy to cellulosic ethanol. *Biofuels, Bioprod. Biorefin, 5*(2), 215–225.

Hamre, A. G., Lorentzen, S. B., Väljamäe, P., & Sorlie, M. (2014). Enzyme processivity changes with the extent of recalcitrant polysaccharide degradation. *FEBS Lett, 588*(24), 4620–4624.

Harjunpää, V., Teleman, A., Koivula, A., Ruohonen, L., Teeri, T. T., Teleman, O., & Drakenberg, T. (1996). Cello-oligosaccharide hydrolysis by cellobiohydrolase II from Trichoderma reesei. Association and rate constants derived from an analysis of progress curves. *Eur J Biochem, 240*(3), 584–591.

Harrison, M. J., Nouwens, A. S., Jardine, D. R., Zachara, N. E., Gooley, A. A., Nevalainen, H., & Packer, N. H. (1998). Modified glycosylation of cellobiohydrolase I from a high cellulase-producing mutant strain of Trichoderma reesei. *Eur J Biochem, 256*(1), 119–127.

Herve, C., Rogowski, A., Blake, A. W., Marcus, S. E., Gilbert, H. J., & Knox, J. P. (2010). Carbohydrate-binding modules promote the enzymatic deconstruction of intact plant cell walls by targeting and proximity effects. *Proc Natl Acad Sci U S A, 107*(34), 15293–15298.

Honda, Y., & Kitaoka, M. (2004). A family 8 glycoside hydrolase from Bacillus halodurans C-125 (BH2105) is a reducing end xylose-releasing exo-oligoxylanase. *J Biol Chem, 279*(53), 55097–55103.

Honda, Y., Taniguchi, H., & Kitaoka, M. (2008). A reducing-end-acting chitinase from Vibrio proteolyticus belonging to glycoside hydrolase family 19. *Appl Microbiol Biotechnol, 78*(4), 627–634.

Horn, S. J., & Eijsink, V. G. (2004). A reliable reducing end assay for chito-oligosaccharides. *Carbohydr Polym, 56*, 35–39.

Horn, S. J., Sikorski, P., Cederkvist, J. B., Vaaje-Kolstad, G., Sorlie, M., Synstad, B., . . . Eijsink, V. G. (2006). Costs and benefits of processivity in enzymatic degradation of recalcitrant polysaccharides. *Proc Natl Acad Sci U S A, 103*(48), 18089–18094.

Horn, S. J., Sorlie, M., Varum, K. M., Väljamäe, P., & Eijsink, V. G. (2012). Measuring processivity. *Methods Enzymol, 510*, 69–95.

Howell, J.A. (1978). Enzyme deactivation during cellulose hydrolysis. *Biotechnol Bioeng, 20*, 847–863.

Howell, JA., & Stuck, JD. (1975). Kinetics of solka floc cellulose hydrolysis by Trichoderma viride cellulase. *Biotechnol Bioeng, 17*, 873–893.

Igarashi, K., Koivula, A., Wada, M., Kimura, S., Penttila, M., & Samejima, M. (2009). High speed atomic force microscopy visualizes processive movement of Trichoderma reesei cellobiohydrolase I on crystalline cellulose. *J Biol Chem, 284*(52), 36186–36190.

Igarashi, K., Uchihashi, T., Koivula, A., Wada, M., Kimura, S., Okamoto, T., . . . Samejima, M. (2011). Traffic jams reduce hydrolytic efficiency of cellulase on cellulose surface. *Science, 333*(6047), 1279–1282.

Imai, T., Boisset, C., Samejima, M., Igarashi, K., & Sugiyama, J. (1998). Unidirectional processive action of cellobiohydrolase Cel7A on Valonia cellulose microcrystals. *FEBS Lett, 432*(3), 113–116.

Irwin, D. C., Spezio, M., Walker, L. P., & Wilson, D. B. (1993). Activity studies of eight purified cellulases: Specificity, synergism, and binding domain effects. *Biotechnol Bioeng, 42*(8), 1002–1013.

Jalak, J., Kurašin, M., Teugjas, H., & Väljamäe, P. (2012). Endo-exo synergism in cellulose hydrolysis revisited. *J Biol Chem, 287*(34), 28802–28815.

Jalak, J., & Väljamäe, P. (2010). Mechanism of initial rapid rate retardation in cellobiohydrolase catalyzed cellulose hydrolysis. *Biotechnol Bioeng, 106*(6), 871–883.

Jalak, J., & Väljamäe, P. (2014). Multi-mode binding of Cellobiohydrolase Cel7A from Trichoderma reesei to cellulose. *PLoS One, 9*(9), e108181.

Kabayama, M.A., Patterson, D., & Piche, L. (1958). The thermodynamics of mutarotation of some sugars I. Measurement of the heat of mutarotation by microcalorimetry. *Can J Chem, 36*(3), 557–562.

Kari, J., Olsen, J., Borch, K., Cruys-Bagger, N., Jensen, K., & Westh, P. (2014). Kinetics of cellobiohydrolase (Cel7A) variants with lowered substrate affinity. *J Biol Chem, 289*(47), 32459–32468.

Karlsson, J., Momcilovic, D., Wittgren, B., Schulein, M., Tjerneld, F., & Brinkmalm, G. (2002). Enzymatic degradation of carboxymethyl cellulose hydrolyzed by the endoglucanases Cel5A, Cel7B, and Cel45A from Humicola insolens and Cel7B, Cel12A and Cel45Acore from Trichoderma reesei. *Biopolymers, 63*(1), 32–40.

Karuna, N., & Jeoh, T. (2017). The productive cellulase binding capacity of cellulosic substrates. *Biotechnol Bioeng, 114*(3), 533–542.

Kern, M., McGeehan, J. E., Streeter, S. D., Martin, R. N., Besser, K., Elias, L., . . . McQueen-Mason, S. J. (2013). Structural characterization of a unique marine animal family 7 cellobiohydrolase suggests a mechanism of cellulase salt tolerance. *Proc Natl Acad Sci U S A, 110*(25), 10189–10194.

Kipper, K., Väljamäe, P., & Johansson, G. (2005). Processive action of cellobiohydrolase Cel7A from Trichoderma reesei is revealed as 'burst' kinetics on fluorescent polymeric model substrates. *Biochem J, 385*(Pt 2), 527–535.

Klemm, D., Heublein, B., Fink, H. P., & Bohn, A. (2005). Cellulose: fascinating biopolymer and sustainable raw material. *Angew Chem Int Ed Engl, 44*(22), 3358–3393.

Kleywegt, G. J., Zou, J. Y., Divne, C., Davies, G. J., Sinning, I., Stahlberg, J., . . . Jones, T. A. (1997). The crystal structure of the catalytic core domain of endoglucanase I from Trichoderma reesei at 3.6 A resolution, and a comparison with related enzymes. *J Mol Biol, 272*(3), 383–397.

Knott, B. C., Crowley, M. F., Himmel, M. E., Stahlberg, J., & Beckham, G. T. (2014a). Carbohydrate-protein interactions that drive processive polysaccharide translocation in enzymes revealed from a computational study of cellobiohydrolase processivity. *J Am Chem Soc, 136*(24), 8810–8819.

Knott, B. C., Haddad Momeni, M., Crowley, M. F., Mackenzie, L. F., Gotz, A. W., Sandgren, M., . . . Beckham, G. T. (2014b). The mechanism of cellulose hydrolysis by a two-step, retaining cellobiohydrolase elucidated by structural and transition path sampling studies. *J Am Chem Soc, 136*(1), 321–329.

Knowles, J.K.C., Lehtovaara, P., Murray, M., & Sinnot, M. L. (1988). Stereochemical course of the action of the cellobiohydrolase I and II of Trrichoderma reesei. *J Chem Soc Chem Commun*, 1401–1402.

Koivula, A., Kinnari, T., Harjunpaa, V., Ruohonen, L., Teleman, A., Drakenberg, T., . . . Teeri, T. T. (1998). Tryptophan 272: an essential determinant of crystalline cellulose

degradation by Trichoderma reesei cellobiohydrolase Cel6A. *FEBS Lett, 429*(3), 341–346.

Koivula, A., Ruohonen, L., Wohlfahrt, G., Reinikainen, T., Teeri, T. T., Piens, K., . . . Jones, T. A. (2002). The active site of cellobiohydrolase Cel6A from Trichoderma reesei: the roles of aspartic acids D221 and D175. *J Am Chem Soc, 124*(34), 10015–10024.

Kont, R., Kurašin, M., Teugjas, H., & Väljamäe, P. (2013). Strong cellulase inhibitors from the hydrothermal pretreatment of wheat straw. *Biotechnol Biofuels, 6*(1), 135.

Koshland, D. E. (1953). Stereochemistry and the mechanism of enzymatic reactions. *Jr. Biol. Rev., 28*, 413.

Kostylev, M., Alahuhta, M., Chen, M., Brunecky, R., Himmel, M. E., Lunin, V. V., . . . Wilson, D. B. (2014). Cel48A from Thermobifida fusca: structure and site directed mutagenesis of key residues. *Biotechnol Bioeng, 111*(4), 664–673.

Kostylev, M., & Wilson, D. (2012). Synergistic interactions in cellulose hydrolysis. *Biofuels, 3*, 61–70.

Kostylev, M., & Wilson, D. (2013). Two-parameter kinetic model based on a time-dependent activity coefficient accurately describes enzymatic cellulose digestion. *Biochemistry, 52*(33), 5656–5664.

Kraulis, J., Clore, G. M., Nilges, M., Jones, T. A., Pettersson, G., Knowles, J., & Gronenborn, A. M. (1989). Determination of the three-dimensional solution structure of the C-terminal domain of cellobiohydrolase I from Trichoderma reesei. A study using nuclear magnetic resonance and hybrid distance geometry-dynamical simulated annealing. *Biochemistry, 28*(18), 7241–7257.

Kurašin, M., Kuusk, S., Kuusk, P., Sorlie, M., & Väljamäe, P. (2015). Slow Off-rates and Strong Product Binding Are Required for Processivity and Efficient Degradation of Recalcitrant Chitin by Family 18 Chitinases. *J Biol Chem, 290*(48), 29074–29085.

Kurašin, M., & Väljamäe, P. (2011). Processivity of cellobiohydrolases is limited by the substrate. *J Biol Chem, 286*(1), 169–177.

Kuusk, S., Sorlie, M., & Väljamäe, P. (2015). The predominant molecular state of bound enzyme determines the strength and type of product inhibition in the hydrolysis of recalcitrant polysaccharides by processive enzymes. *J Biol Chem, 290*(18), 11678–11691.

Lee, Y. H., & Fan, L. T. (1982). Kinetic studies of enzymatic hydrolysis of insoluble cellulose: analysis of the initial rates. *Biotechnol Bioeng, 24*(11), 2383–2406.

Li, Y., Irwin, D. C., & Wilson, D. B. (2007). Processivity, substrate binding, and mechanism of cellulose hydrolysis by Thermobifida fusca Cel9A. *Appl Environ Microbiol, 73*(10), 3165–3172.

Lombard, V., Golaconda Ramulu, H., Drula, E., Coutinho, P. M., & Henrissat, B. (2014). The carbohydrate-active enzymes database (CAZy) in 2013. *Nucleic Acids Res, 42*(Database issue), D490–495.

Lynd, L. R., Laser, M. S., Bransby, D., Dale, B. E., Davison, B., Hamilton, R., . . . Wyman, C. E. (2008). How biotech can transform biofuels. *Nat Biotechnol, 26*(2), 169–172.

McLean, B. W., Boraston, A. B., Brouwer, D., Sanaie, N., Fyfe, C. A., Warren, R. A., . . . Haynes, C. A. (2002). Carbohydrate-binding modules recognize fine substructures of cellulose. *J Biol Chem, 277*(52), 50245–50254.

Medve, J., Karlsson, J., Lee, D., & Tjerneld, F. (1998). Hydrolysis of microcrystalline cellulose by cellobiohydrolase I and endoglucanase II from Trichoderma reesei:

adsorption, sugar production pattern, and synergism of the enzymes. *Biotechnol Bioeng, 59*(5), 621–634.

Morgenstern, I., Powlowski, J., & Tsang, A. (2014). Fungal cellulose degradation by oxidative enzymes: from dysfunctional GH61 family to powerful lytic polysaccharide monooxygenase family. *Brief Funct Genomics, 13*(6), 471–481.

Murphy, L., Bohlin, C., Baumann, M. J., Olsen, S. N., Sorensen, T. H., Anderson, L., . . . Westh, P. (2013). Product inhibition of five Hypocrea jecorina cellulases. *Enzyme Microb Technol, 52*(3), 163–169.

Nakamura, A., Tasaki, T., Ishiwata, D., Yamamoto, M., Okuni, Y., Visootsat, A., . . . Iino, R. (2016). Single-molecule Imaging Analysis of Binding, Processive Movement, and Dissociation of Cellobiohydrolase Trichoderma reesei Cel6A and Its Domains on Crystalline Cellulose. *J Biol Chem, 291*(43), 22404–22413.

Nakamura, A., Tsukada, T., Auer, S., Furuta, T., Wada, M., Koivula, A., . . . Samejima, M. (2013). The tryptophan residue at the active site tunnel entrance of Trichoderma reesei cellobiohydrolase Cel7A is important for initiation of degradation of crystalline cellulose. *J Biol Chem, 288*(19), 13503–13510.

Nakamura, A., Watanabe, H., Ishida, T., Uchihashi, T., Wada, M., Ando, T., . . . Samejima, M. (2014). Trade-off between processivity and hydrolytic velocity of cellobiohydrolases at the surface of crystalline cellulose. *J Am Chem Soc, 136*(12), 4584–4592.

Navard, P., & Cuissinat, C. (2006). Cellulose swelling and dissolution as a tool to study the fiber structure. *7th International Symposium "Alternative Cellulose: Manufacturing, Forming, Properties"*.

Nidetzky, B., Zachariae, W., Gercken, G., Hayn, M., & Steiner, W. (1994). Hydrolysis of cellooligosaccharides by Trichoderma reesei cellobiohydrolases: Experimental data and kinetic modelling. *Enzyme Microb Technol, 16*, 43–52.

Nimlos, M. R., Beckham, G. T., Matthews, J. F., Bu, L., Himmel, M. E., & Crowley, M. F. (2012). Binding preferences, surface attachment, diffusivity, and orientation of a family 1 carbohydrate-binding module on cellulose. *J Biol Chem, 287*(24), 20603–20612.

Nishiyama, Y., Langan, P., & Chanzy, H. (2002). Crystal structure and hydrogen-bonding system in cellulose Ibeta from synchrotron X-ray and neutron fiber diffraction. *J Am Chem Soc, 124*(31), 9074–9082.

Nishiyama, Y., Sugiyama, J., Chanzy, H., & Langan, P. (2003). Crystal structure and hydrogen bonding system in cellulose I(alpha) from synchrotron X-ray and neutron fiber diffraction. *J Am Chem Soc, 125*(47), 14300–14306.

Nutt, A., Sild, V., Pettersson, G., & Johansson, G. (1998). Progress curves – a mean for functional classification of cellulases. *Eur J Biochem, 258*(1), 200–206.

Olsen, J. P., Alasepp, K., Kari, J., Cruys-Bagger, N., Borch, K., & Westh, P. (2016). Mechanism of product inhibition for cellobiohydrolase Cel7A during hydrolysis of insoluble cellulose. *Biotechnol Bioeng, 113*(6), 1178–1186.

Park, Y. B., & Cosgrove, D. J. (2012). A revised architecture of primary cell walls based on biomechanical changes induced by substrate-specific endoglucanases. *Plant Physiol, 158*(4), 1933–1943.

Pauly, M., & Keegstra, K. (2008). Cell-wall carbohydrates and their modification as a resource for biofuels. *Plant J, 54*(4), 559–568.

Payne, C. M., Bomble, Y. J., Taylor, C. B., McCabe, C., Himmel, M. E., Crowley, M. F., & Beckham, G. T. (2011). Multiple functions of aromatic-carbohydrate interactions

in a processive cellulase examined with molecular simulation. *J Biol Chem, 286*(47), 41028–41035.

Payne, C. M., Jiang, W., Shirts, M. R., Himmel, M. E., Crowley, M. F., & Beckham, G. T. (2013a). Glycoside hydrolase processivity is directly related to oligosaccharide binding free energy. *J Am Chem Soc, 135*(50), 18831–18839.

Payne, C. M., Knott, B. C., Mayes, H. B., Hansson, H., Himmel, M. E., Sandgren, M., . . . Beckham, G. T. (2015). Fungal cellulases. *Chem Rev, 115*(3), 1308–1448.

Payne, C. M., Resch, M. G., Chen, L., Crowley, M. F., Himmel, M. E., Taylor, L. E., 2nd, . . . Beckham, G. T. (2013b). Glycosylated linkers in multimodular lignocellulose-degrading enzymes dynamically bind to cellulose. *Proc Natl Acad Sci U S A, 110*(36), 14646–14651.

Peterson, R., & Nevalainen, H. (2012). Trichoderma reesei RUT-C30 – thirty years of strain improvement. *Microbiology, 158*(Pt 1), 58–68.

Praestgaard, E., Elmerdahl, J., Murphy, L., Nymand, S., McFarland, K. C., Borch, K., & Westh, P. (2011). A kinetic model for the burst phase of processive cellulases. *FEBS J, 278*(9), 1547–1560.

Quinlan, R. J., Sweeney, M. D., Lo Leggio, L., Otten, H., Poulsen, J. C., Johansen, K. S., . . . Walton, P. H. (2011). Insights into the oxidative degradation of cellulose by a copper metalloenzyme that exploits biomass components. *Proc Natl Acad Sci U S A, 108*(37), 15079–15084.

Sammond, D. W., Payne, C. M., Brunecky, R., Himmel, M. E., Crowley, M. F., & Beckham, G. T. (2012). Cellulase linkers are optimized based on domain type and function: insights from sequence analysis, biophysical measurements, and molecular simulation. *PLoS One, 7*(11), e48615.

Sandgren, M., Shaw, A., Ropp, T. H., Wu, S., Bott, R., Cameron, A. D., . . . Jones, T. A. (2001). The X-ray crystal structure of the Trichoderma reesei family 12 endoglucanase 3, Cel12A, at 1.9 A resolution. *J Mol Biol, 308*(2), 295–310.

Schou, C., Rasmussen, G., Kaltoft, M. B., Henrissat, B., & Schulein, M. (1993). Stereochemistry, specificity and kinetics of the hydrolysis of reduced cellodextrins by nine cellulases. *Eur J Biochem, 217*(3), 947–953.

Srisodsuk, M., Reinikainen, T., Penttila, M., & Teeri, T. T. (1993). Role of the interdomain linker peptide of Trichoderma reesei cellobiohydrolase I in its interaction with crystalline cellulose. *J Biol Chem, 268*(28), 20756–20761.

Stahlberg, J., Divne, C., Koivula, A., Piens, K., Claeyssens, M., Teeri, T. T., & Jones, T. A. (1996). Activity studies and crystal structures of catalytically deficient mutants of cellobiohydrolase I from Trichoderma reesei. *J Mol Biol, 264*(2), 337–349.

Stahlberg, J., Johansson, G., & Pettersson, G. (1993). Trichoderma reesei has no true exo-cellulase: all intact and truncated cellulases produce new reducing end groups on cellulose. *Biochim Biophys Acta, 1157*(1), 107–113.

Ståhlberg, J., Johansson, G., & Pettersson, G. . (1991). A new model for enzymatic hydrolysis of cellulose based on the two-domain structure of cellobiohydrolase I. *Nat Biotechnol, 9*, 286–290.

Stals, I., Sandra, K., Geysens, S., Contreras, R., Van Beeumen, J., & Claeyssens, M. (2004). Factors influencing glycosylation of Trichoderma reesei cellulases. I: Post-secretorial changes of the O- and N-glycosylation pattern of Cel7A. *Glycobiology, 14*(8), 713–724.

Sugimoto, N., Igarashi, K., Wada, M., & Samejima, M. (2012). Adsorption characteristics of fungal family 1 cellulose-binding domain from Trichoderma reesei cello-

biohydrolase I on crystalline cellulose: negative cooperative adsorption via a steric exclusion effect. *Langmuir, 28*(40), 14323–14329.

Suginta, W., Pantoom, S., & Prinz, H. (2009). Substrate binding modes and anomer selectivity of chitinase A from Vibrio harveyi. *J Chem Biol, 2*(4), 191–202.

Suominen, P. L., Mantyla, A. L., Karhunen, T., Hakola, S., & Nevalainen, H. (1993). High frequency one-step gene replacement in Trichoderma reesei. II. Effects of deletions of individual cellulase genes. *Mol Gen Genet, 241*(5–6), 523–530.

Taylor, C. B., Payne, C. M., Himmel, M. E., Crowley, M. F., McCabe, C., & Beckham, G. T. (2013). Binding site dynamics and aromatic-carbohydrate interactions in processive and non-processive family 7 glycoside hydrolases. *J Phys Chem B, 117*(17), 4924–4933.

Teeri, T. T., Koivula, A., Linder, M., Wohlfahrt, G., Divne, C., & Jones, T. A. (1998). Trichoderma reesei cellobiohydrolases: why so efficient on crystalline cellulose? *Biochem Soc Trans, 26*(2), 173–178.

Terinte, N., Ibbett, R., & Schuster, K.C. (2011). Overview on native cellulose and microcrystalline cellulose I structure studied by X-ray diffraction (WAXD): Comparison between measurement techniques. *Lenzinger Berichte, 89*, 118–131.

Teugjas, H., & Väljamäe, P. (2013). Product inhibition of cellulases studied with 14C-labeled cellulose substrates. *Biotechnol Biofuels, 6*(1), 104.

Textor, L. C., Colussi, F., Silveira, R. L., Serpa, V., de Mello, B. L., Muniz, J. R., . . . Polikarpov, I. (2013). Joint X-ray crystallographic and molecular dynamics study of cellobiohydrolase I from Trichoderma harzianum: deciphering the structural features of cellobiohydrolase catalytic activity. *FEBS J, 280*(1), 56–69.

Tuohy, M. G., Walsh, D. J., Murray, P. G., Claeyssens, M., Cuffe, M. M., Savage, A. V., & Coughlan, M. P. (2002). Kinetic parameters and mode of action of the cellobiohydrolases produced by Talaromyces emersonii. *Biochim Biophys Acta, 1596*(2), 366–380.

Ubhayasekera, W., Munoz, I. G., Vasella, A., Stahlberg, J., & Mowbray, S. L. (2005). Structures of Phanerochaete chrysosporium Cel7D in complex with product and inhibitors. *FEBS J, 272*(8), 1952–1964.

Ülker, A., & Sprey, B. (1990). Characterization of an unglycosylated low molecular weight 1,4-beta-glucan-glucanohydrolase of Trichoderma reesei. *FEMS Microbiol Lett, 57*(3), 215–219.

Vaaje-Kolstad, G., Westereng, B., Horn, S. J., Liu, Z., Zhai, H., Sorlie, M., & Eijsink, V. G. (2010). An oxidative enzyme boosting the enzymatic conversion of recalcitrant polysaccharides. *Science, 330*(6001), 219–222.

Väljamäe, P., Sild, V., Nutt, A., Pettersson, G., & Johansson, G. (1999). Acid hydrolysis of bacterial cellulose reveals different modes of synergistic action between cellobiohydrolase I and endoglucanase I. *Eur J Biochem, 266*(2), 327–334.

van Tilbeurgh, H., & Claeyssens, M. (1985). Detection and differentiation of cellulase components using low molecular mass fluorogenic substrates. *FEBS Letters, 187*, 283–288.

Várnai, A., Siika-aho, M., & Viikari, L. (2010). Restriction of the enzymatic hydrolysis of steam-pretreated spruce by lignin and hemicellulose. *Enzyme Microb Technol 46*, 185–193.

Várnai, A., Siika-Aho, M., & Viikari, L. (2013). Carbohydrate-binding modules (CBMs) revisited: reduced amount of water counterbalances the need for CBMs. *Biotechnol Biofuels, 6*(1), 30.

von Ossowski, I., Stahlberg, J., Koivula, A., Piens, K., Becker, D., Boer, H., . . . Teeri, T. T. (2003). Engineering the exo-loop of Trichoderma reesei cellobiohydrolase, Cel7A. A comparison with Phanerochaete chrysosporium Cel7D. *J Mol Biol, 333*(4), 817–829.

Voutilainen, S. P., Puranen, T., Siika-Aho, M., Lappalainen, A., Alapuranen, M., Kallio, J., . . . Koivula, A. (2008). Cloning, expression, and characterization of novel thermostable family 7 cellobiohydrolases. *Biotechnol Bioeng, 101*(3), 515–528.

Vrsanska, M., & Biely, P. (1992). The cellobiohydrolase-I from Trichoderma-reesei Qm-9414 – action on cellooligosaccharides. *Carbohydr Res, 227*, 19–27.

Vuong, T. V., & Wilson, D. B. (2009). Processivity, synergism, and substrate specificity of Thermobifida fusca Cel6B. *Appl Environ Microbiol, 75*(21), 6655–6661.

Wang, Y., Zhang, S., Song, X., & Yao, L. (2016). Cellulose chain binding free energy drives the processive move of cellulases on the cellulose surface. *Biotechnol Bioeng, 113*(9), 1873–1880.

Wood, T. M., & McCrae, S. I. (1972). The purification and properties of the C 1 component of Trichoderma koningii cellulase. *Biochem J, 128*(5), 1183–1192.

Woodward, J. (1991). Synergism in cellulase systems. . *Bioresour Technol, 36*, 67–75.

Wyman, C. E. (2001). Twenty years of trials, tribulations, and research progress in bioethanol technology: selected key events along the way. *Appl Biochem Biotechnol, 91–93*, 5–21.

Yang, B., & Wyman, C. E. (2008). Pretreatment: the key to unlocking low-cost cellulosic ethanol *Biofuels, Bioprod. Biorefin, 2*, 26–40.

Yuan, S., Wu, Y., & Cosgrove, D. J. (2001). A fungal endoglucanase with plant cell wall extension activity. *Plant Physiol, 127*(1), 324–333.

Zakariassen, H., Aam, B. B., Horn, S. J., Varum, K. M., Sorlie, M., & Eijsink, V. G. (2009). Aromatic residues in the catalytic center of chitinase A from Serratia marcescens affect processivity, enzyme activity, and biomass converting efficiency. *J Biol Chem, 284*(16), 10610–10617.

Zhang, S., Irwin, D. C., & Wilson, D. B. (2000). Site-directed mutation of noncatalytic residues of Thermobifida fusca exocellulase Cel6B. *Eur J Biochem, 267*(11), 3101–3115.

Zhang, Y. H. P., Cui, J. B., Lynd, L. R., & Kuang, L. R. (2006). A transition from cellulose swelling to cellulose dissolution by o-phosphoric acid: Evidence from enzymatic hydrolysis and supramolecular structure. *Biomacromolecules, 7*(2), 644–648.

Zou, J., Kleywegt, G. J., Stahlberg, J., Driguez, H., Nerinckx, W., Claeyssens, M., . . . Jones, T. A. (1999). Crystallographic evidence for substrate ring distortion and protein conformational changes during catalysis in cellobiohydrolase Ce16A from trichoderma reesei. *Structure, 7*(9), 1035–1045.

Zverlov, V. V., Velikodvorskaya, G. A., & Schwarz, W. H. (2002). A newly described cellulosomal cellobiohydrolase, CelO, from Clostridium thermocellum: investigation of the exo-mode of hydrolysis, and binding capacity to crystalline cellulose. *Microbiology, 148*(Pt 1), 247–255.

ACKNOWLEDGMENTS

I thank all who have helped and contributed to making it happen! First and foremost, I thank my supervisor Priit Väljamäe for his calm and always supportive supervision. I feel that Priit is the one who equilibrates my restless mind and have helped to translate my thoughts and doings into scientific language. I am thankful for the opportunity of being involved and supervised from the beginning until the end of my long way as a student in academia!

I would like to thank Silja for the company in the lab and for the talks about science, children and the ways of looking at things. Also, thank you Silja for making my writings more accessible and easier to read. I thank my lab mates Jürgen and Mihhail for shearing all the joys and concerns of doing research during all these years. It has been a great pleasure of being part of the group of the 2nd floor at Omicum! I thank all the colleagues, especially Aivar, Jaanus, Joachim, Juhan, Ilja, Maie, Margus, Mikk, Priit J., Tiina S., and Tiina T. for being surrounded by a good company, food smells and tastes, and joy. Thank you Aivar for showing that taking calm and easy is the key to work it out!

I am also grateful to Tiina Alamäe for proofreading my thesis. Her useful suggestions and improvements adjusted the quality of the thesis, and the optimistic attitude boosted me with confidence that the defence will finally become realistic.

I would also like to thank the co-authors of the publications for the fruitful collaboration. I still wonder that the paper about anomer-selectivity really became true and special thanks for it to Jeppe Kari and Peter Westh.

Still, I feel that one important piece is absent from my theses – the oligosaccharidic inhibitors. From all of the research done, this was the most favoured and educative topic for me. These inhibitors were the reason why I faced with mass spectrometry and protein crystallography. Although the inhibitor-protein complexes did not work out and I turned on my way, I am thankful to the crystallography team at Swedish University of Agricultural Sciences, especially to Jerry Stahlberg, Anna Borisova and Mats Sandgren. Thank you Jerry for introducing me the principles and the beauty of crystallography and for colouring my protein world. Thank you Anna for the time spent together here and there, hurrah for bicycle-like Cel7As!

I thank all my dear friends for your mental support, understanding and listening. Thank you Laura for pushing me back to start the studies in Tartu, I think neither of us did not imagine that it would turn out like that.

At last, I would like to thank my family. Specially Raido for the absolute love and support. Thank you for shearing the parental care and giving me the time to concentrate on research. Thank you Marta and Mari for the feeling that I am a beloved mother, time together with you brings out the Sun. Thank you my dear parents for your understanding and believing in me, and for the freedom to make decisions. I am thankful to the whole family clan for supporting me and encouraging through all these years.

PUBLICATIONS

CURRICULUM VITAE

Name: Riin Kont (Velleste)
Date of birth: 18.05.1987
Citizenship: Estonian
Address: Institute of Molecular and Cell Biology, University of Tartu
Riia 23C, 51010, Tartu, Estonia
E-mail: riin.kont@ut.ee

Education:

2013– University of Tartu, doctorate studies, molecular biology
2010–2013 University of Tartu, MSc, molecular biology *(cum laude)*
2006–2010 University of Tartu, BSc, biology
2003–2006 Tallinn Secondary School of Science

Language skills: Estonian (native); English, Russian

Professional employment:

2011–2017 University of Tartu, Institute of Molecular and Cell Biology, specialist

List of publications:

Kari J., Kont R., Borch K., Buskov S., Olsen J.P., Cruyz-Bagger N., Väljamäe P., Westh P. (2017) Anomeric selectivity and product profile of a processive cellulase. Biochemistry 56(1):167–178

Kont R., Kari J., Borch K., Westh P., Väljamäe P. (2016) Inter-domain synergism is required for efficient feeding of cellulose chain into active site of cellobiohydrolase Cel7A. J Biol Chem. 291(50):26013–26023

Kont R., Kurashin M., Teugjas H., Väljamäe P. (2013) Strong cellulase inhibitors from the hydrothermal pretreatment of wheat straw. Biotechnology for Biofuels 6:135

Velleste R., Teugjas H., Väljamäe P. (2010). Reducing end-specific fluorescence labeled celluloses for cellulase mode of action. Cellulose 17 (1): 125−138

Membership in professional organizations:

Student member of the Estonian Biochemical Society

ELULOOKIRJELDUS

Nimi: Riin Kont (Velleste)
Sünniaeg: 18.05.1987
Kodakondsus: Eesti
Aadress: Molekulaar- ja Rakubioloogia Instituut, Tartu Ülikool, Riia 23C, 51010, Tartu, Eesti
E-post: riin.kont@ut.ee

Haridus:

2013–. . . Tartu Ülikool, doktoriõpe, molekulaarbioloogia erialal,
2010–2013 Tartu Ülikool, MSc molekulaarbioloogia erialal (cum laude),
2006–2010 Tartu Ülikool, BSc bioloogia erialal
2003–2006 Tallinna Reaalkool

Keelteoskus: eesti (emakeel), inglise, vene

Töökogemus:

2011–2017 Tartu Ülikool, Molekulaar- ja Rakubioloogia Instituut, spetsialist

Publikatsioonid

Kari J., Kont R., Borch K., Buskov S., Olsen J.P., Cruys-Bagger N., Väljamäe P., Westh P. (2017) Anomeric selectivity and product profile of a processive cellulase. Biochemistry 56(1): 167–178.

Kont R., Kari J., Borch K., Westh P., Väljamäe P. (2016) Inter-domain synergism is required for efficient feeding of cellulose chain into active site of cellobiohydrolase Cel7A. J Biol Chem. 291(50): 26013–26023.

Kont R., Kurašin M., Teugjas H., Väljamäe P. (2013) Strong cellulase inhibitors from the hydrothermal pretreatment of wheat straw. Biotechnol Biofuels 6:135

Velleste R., Teugjas H., Väljamäe P. (2010) Reducing end-specific fluorescence labeled celluloses for cellulase mode of action. Cellulose 17(1): 125–138

Erialaline liikmelisus:

Eesti Biokeemia Seltsi üliõpilasliige

DISSERTATIONES BIOLOGICAE UNIVERSITATIS TARTUENSIS

1. **Toivo Maimets**. Studies of human oncoprotein p53. Tartu, 1991, 96 p.
2. **Enn K. Seppet**. Thyroid state control over energy metabolism, ion transport and contractile functions in rat heart. Tartu, 1991, 135 p.
3. **Kristjan Zobel**. Epifüütsete makrosamblike väärtus õhu saastuse indikaatoritena Hamar-Dobani boreaalsetes mägimetsades. Tartu, 1992, 131 lk.
4. **Andres Mäe**. Conjugal mobilization of catabolic plasmids by transposable elements in helper plasmids. Tartu, 1992, 91 p.
5. **Maia Kivisaar**. Studies on phenol degradation genes of *Pseudomonas* sp. strain EST 1001. Tartu, 1992, 61 p.
6. **Allan Nurk**. Nucleotide sequences of phenol degradative genes from *Pseudomonas sp.* strain EST 1001 and their transcriptional activation in *Pseudomonas putida.* Tartu, 1992, 72 p.
7. **Ülo Tamm**. The genus *Populus* L. in Estonia: variation of the species biology and introduction. Tartu, 1993, 91 p.
8. **Jaanus Remme**. Studies on the peptidyltransferase centre of the *E.coli* ribosome. Tartu, 1993, 68 p.
9. **Ülo Langel**. Galanin and galanin antagonists. Tartu, 1993, 97 p.
10. **Arvo Käärd**. The development of an automatic online dynamic fluorescense-based pH-dependent fiber optic penicillin flowthrought biosensor for the control of the benzylpenicillin hydrolysis. Tartu, 1993, 117 p.
11. **Lilian Järvekülg**. Antigenic analysis and development of sensitive immunoassay for potato viruses. Tartu, 1993, 147 p.
12. **Jaak Palumets**. Analysis of phytomass partition in Norway spruce. Tartu, 1993, 47 p.
13. **Arne Sellin**. Variation in hydraulic architecture of *Picea abies* (L.) Karst. trees grown under different enviromental conditions. Tartu, 1994, 119 p.
13. **Mati Reeben**. Regulation of light neurofilament gene expression. Tartu, 1994, 108 p.
14. **Urmas Tartes**. Respiration rhytms in insects. Tartu, 1995, 109 p.
15. **Ülo Puurand**. The complete nucleotide sequence and infections *in vitro* transcripts from cloned cDNA of a potato A potyvirus. Tartu, 1995, 96 p.
16. **Peeter Hõrak**. Pathways of selection in avian reproduction: a functional framework and its application in the population study of the great tit (*Parus major*). Tartu, 1995, 118 p.
17. **Erkki Truve**. Studies on specific and broad spectrum virus resistance in transgenic plants. Tartu, 1996, 158 p.
18. **Illar Pata**. Cloning and characterization of human and mouse ribosomal protein S6-encoding genes. Tartu, 1996, 60 p.
19. **Ülo Niinemets**. Importance of structural features of leaves and canopy in determining species shade-tolerance in temperature deciduous woody taxa. Tartu, 1996, 150 p.

20. **Ants Kurg**. Bovine leukemia virus: molecular studies on the packaging region and DNA diagnostics in cattle. Tartu, 1996, 104 p.
21. **Ene Ustav**. E2 as the modulator of the BPV1 DNA replication. Tartu, 1996, 100 p.
22. **Aksel Soosaar**. Role of helix-loop-helix and nuclear hormone receptor transcription factors in neurogenesis. Tartu, 1996, 109 p.
23. **Maido Remm**. Human papillomavirus type 18: replication, transformation and gene expression. Tartu, 1997, 117 p.
24. **Tiiu Kull**. Population dynamics in *Cypripedium calceolus* L. Tartu, 1997, 124 p.
25. **Kalle Olli**. Evolutionary life-strategies of autotrophic planktonic microorganisms in the Baltic Sea. Tartu, 1997, 180 p.
26. **Meelis Pärtel**. Species diversity and community dynamics in calcareous grassland communities in Western Estonia. Tartu, 1997, 124 p.
27. **Malle Leht**. The Genus *Potentilla* L. in Estonia, Latvia and Lithuania: distribution, morphology and taxonomy. Tartu, 1997, 186 p.
28. **Tanel Tenson**. Ribosomes, peptides and antibiotic resistance. Tartu, 1997, 80 p.
29. **Arvo Tuvikene**. Assessment of inland water pollution using biomarker responses in fish *in vivo* and *in vitro*. Tartu, 1997, 160 p.
30. **Urmas Saarma**. Tuning ribosomal elongation cycle by mutagenesis of 23S rRNA. Tartu, 1997, 134 p.
31. **Henn Ojaveer**. Composition and dynamics of fish stocks in the gulf of Riga ecosystem. Tartu, 1997, 138 p.
32. **Lembi Lõugas**. Post-glacial development of vertebrate fauna in Estonian water bodies. Tartu, 1997, 138 p.
33. **Margus Pooga**. Cell penetrating peptide, transportan, and its predecessors, galanin-based chimeric peptides. Tartu, 1998, 110 p.
34. **Andres Saag**. Evolutionary relationships in some cetrarioid genera (Lichenized Ascomycota). Tartu, 1998, 196 p.
35. **Aivar Liiv**. Ribosomal large subunit assembly *in vivo*. Tartu, 1998, 158 p.
36. **Tatjana Oja**. Isoenzyme diversity and phylogenetic affinities among the eurasian annual bromes (*Bromus* L., Poaceae). Tartu, 1998, 92 p.
37. **Mari Moora**. The influence of arbuscular mycorrhizal (AM) symbiosis on the competition and coexistence of calcareous grassland plant species. Tartu, 1998, 78 p.
38. **Olavi Kurina**. Fungus gnats in Estonia (*Diptera: Bolitophilidae, Keroplatidae, Macroceridae, Ditomyiidae, Diadocidiidae, Mycetophilidae*). Tartu, 1998, 200 p.
39. **Andrus Tasa**. Biological leaching of shales: black shale and oil shale. Tartu, 1998, 98 p.
40. **Arnold Kristjuhan**. Studies on transcriptional activator properties of tumor suppressor protein p53. Tartu, 1998, 86 p.
41. **Sulev Ingerpuu**. Characterization of some human myeloid cell surface and nuclear differentiation antigens. Tartu, 1998, 163 p.

42. **Veljo Kisand**. Responses of planktonic bacteria to the abiotic and biotic factors in the shallow lake Võrtsjärv. Tartu, 1998, 118 p.
43. **Kadri Põldmaa**. Studies in the systematics of hypomyces and allied genera (Hypocreales, Ascomycota). Tartu, 1998, 178 p.
44. **Markus Vetemaa**. Reproduction parameters of fish as indicators in environmental monitoring. Tartu, 1998, 117 p.
45. **Heli Talvik**. Prepatent periods and species composition of different *Oesophagostomum* spp. populations in Estonia and Denmark. Tartu, 1998, 104 p.
46. **Katrin Heinsoo**. Cuticular and stomatal antechamber conductance to water vapour diffusion in *Picea abies* (L.) karst. Tartu, 1999, 133 p.
47. **Tarmo Annilo**. Studies on mammalian ribosomal protein S7. Tartu, 1998, 77 p.
48. **Indrek Ots**. Health state indicies of reproducing great tits (*Parus major*): sources of variation and connections with life-history traits. Tartu, 1999, 117 p.
49. **Juan Jose Cantero**. Plant community diversity and habitat relationships in central Argentina grasslands. Tartu, 1999, 161 p.
50. **Rein Kalamees**. Seed bank, seed rain and community regeneration in Estonian calcareous grasslands. Tartu, 1999, 107 p.
51. **Sulev Kõks**. Cholecystokinin (CCK) – induced anxiety in rats: influence of environmental stimuli and involvement of endopioid mechanisms and serotonin. Tartu, 1999, 123 p.
52. **Ebe Sild**. Impact of increasing concentrations of O_3 and CO_2 on wheat, clover and pasture. Tartu, 1999, 123 p.
53. **Ljudmilla Timofejeva**. Electron microscopical analysis of the synaptonemal complex formation in cereals. Tartu, 1999, 99 p.
54. **Andres Valkna**. Interactions of galanin receptor with ligands and G-proteins: studies with synthetic peptides. Tartu, 1999, 103 p.
55. **Taavi Virro**. Life cycles of planktonic rotifers in lake Peipsi. Tartu, 1999, 101 p.
56. **Ana Rebane**. Mammalian ribosomal protein S3a genes and intron-encoded small nucleolar RNAs U73 and U82. Tartu, 1999, 85 p.
57. **Tiina Tamm**. Cocksfoot mottle virus: the genome organisation and translational strategies. Tartu, 2000, 101 p.
58. **Reet Kurg**. Structure-function relationship of the bovine papilloma virus E2 protein. Tartu, 2000, 89 p.
59. **Toomas Kivisild**. The origins of Southern and Western Eurasian populations: an mtDNA study. Tartu, 2000, 121 p.
60. **Niilo Kaldalu**. Studies of the TOL plasmid transcription factor XylS. Tartu, 2000, 88 p.
61. **Dina Lepik**. Modulation of viral DNA replication by tumor suppressor protein p53. Tartu, 2000, 106 p.

62. **Kai Vellak**. Influence of different factors on the diversity of the bryophyte vegetation in forest and wooded meadow communities. Tartu, 2000, 122 p.
63. **Jonne Kotta**. Impact of eutrophication and biological invasionas on the structure and functions of benthic macrofauna. Tartu, 2000, 160 p.
64. **Georg Martin**. Phytobenthic communities of the Gulf of Riga and the inner sea the West-Estonian archipelago. Tartu, 2000, 139 p.
65. **Silvia Sepp**. Morphological and genetical variation of *Alchemilla L.* in Estonia. Tartu, 2000. 124 p.
66. **Jaan Liira**. On the determinants of structure and diversity in herbaceous plant communities. Tartu, 2000, 96 p.
67. **Priit Zingel**. The role of planktonic ciliates in lake ecosystems. Tartu, 2001, 111 p.
68. **Tiit Teder**. Direct and indirect effects in Host-parasitoid interactions: ecological and evolutionary consequences. Tartu, 2001, 122 p.
69. **Hannes Kollist**. Leaf apoplastic ascorbate as ozone scavenger and its transport across the plasma membrane. Tartu, 2001, 80 p.
70. **Reet Marits**. Role of two-component regulator system PehR-PehS and extracellular protease PrtW in virulence of *Erwinia Carotovora* subsp. *Carotovora*. Tartu, 2001, 112 p.
71. **Vallo Tilgar**. Effect of calcium supplementation on reproductive performance of the pied flycatcher *Ficedula hypoleuca* and the great tit *Parus major,* breeding in Nothern temperate forests. Tartu, 2002, 126 p.
72. **Rita Hõrak**. Regulation of transposition of transposon Tn*4652* in *Pseudomonas putida*. Tartu, 2002, 108 p.
73. **Liina Eek-Piirsoo**. The effect of fertilization, mowing and additional illumination on the structure of a species-rich grassland community. Tartu, 2002, 74 p.
74. **Krõõt Aasamaa**. Shoot hydraulic conductance and stomatal conductance of six temperate deciduous tree species. Tartu, 2002, 110 p.
75. **Nele Ingerpuu**. Bryophyte diversity and vascular plants. Tartu, 2002, 112 p.
76. **Neeme Tõnisson**. Mutation detection by primer extension on oligonucleotide microarrays. Tartu, 2002, 124 p.
77. **Margus Pensa**. Variation in needle retention of Scots pine in relation to leaf morphology, nitrogen conservation and tree age. Tartu, 2003, 110 p.
78. **Asko Lõhmus**. Habitat preferences and quality for birds of prey: from principles to applications. Tartu, 2003, 168 p.
79. **Viljar Jaks**. p53 – a switch in cellular circuit. Tartu, 2003, 160 p.
80. **Jaana Männik**. Characterization and genetic studies of four ATP-binding cassette (ABC) transporters. Tartu, 2003, 140 p.
81. **Marek Sammul**. Competition and coexistence of clonal plants in relation to productivity. Tartu, 2003, 159 p
82. **Ivar Ilves**. Virus-cell interactions in the replication cycle of bovine papillomavirus type 1. Tartu, 2003, 89 p.

83. **Andres Männik**. Design and characterization of a novel vector system based on the stable replicator of bovine papillomavirus type 1. Tartu, 2003, 109 p.
84. **Ivika Ostonen**. Fine root structure, dynamics and proportion in net primary production of Norway spruce forest ecosystem in relation to site conditions. Tartu, 2003, 158 p.
85. **Gudrun Veldre**. Somatic status of 12–15-year-old Tartu schoolchildren. Tartu, 2003, 199 p.
86. **Ülo Väli**. The greater spotted eagle *Aquila clanga* and the lesser spotted eagle *A. pomarina*: taxonomy, phylogeography and ecology. Tartu, 2004, 159 p.
87. **Aare Abroi**. The determinants for the native activities of the bovine papillomavirus type 1 E2 protein are separable. Tartu, 2004, 135 p.
88. **Tiina Kahre**. Cystic fibrosis in Estonia. Tartu, 2004, 116 p.
89. **Helen Orav-Kotta**. Habitat choice and feeding activity of benthic suspension feeders and mesograzers in the northern Baltic Sea. Tartu, 2004, 117 p.
90. **Maarja Öpik**. Diversity of arbuscular mycorrhizal fungi in the roots of perennial plants and their effect on plant performance. Tartu, 2004, 175 p.
91. **Kadri Tali**. Species structure of *Neotinea ustulata*. Tartu, 2004, 109 p.
92. **Kristiina Tambets**. Towards the understanding of post-glacial spread of human mitochondrial DNA haplogroups in Europe and beyond: a phylogeographic approach. Tartu, 2004, 163 p.
93. **Arvi Jõers**. Regulation of p53-dependent transcription. Tartu, 2004, 103 p.
94. **Lilian Kadaja**. Studies on modulation of the activity of tumor suppressor protein p53. Tartu, 2004, 103 p.
95. **Jaak Truu**. Oil shale industry wastewater: impact on river microbial community and possibilities for bioremediation. Tartu, 2004, 128 p.
96. **Maire Peters**. Natural horizontal transfer of the *pheBA* operon. Tartu, 2004, 105 p.
97. **Ülo Maiväli**. Studies on the structure-function relationship of the bacterial ribosome. Tartu, 2004, 130 p.
98. **Merit Otsus**. Plant community regeneration and species diversity in dry calcareous grasslands. Tartu, 2004, 103 p.
99. **Mikk Heidemaa**. Systematic studies on sawflies of the genera *Dolerus, Empria,* and *Caliroa* (Hymenoptera: Tenthredinidae). Tartu, 2004, 167 p.
100. **Ilmar Tõnno**. The impact of nitrogen and phosphorus concentration and N/P ratio on cyanobacterial dominance and N_2 fixation in some Estonian lakes. Tartu, 2004, 111 p.
101. **Lauri Saks**. Immune function, parasites, and carotenoid-based ornaments in greenfinches. Tartu, 2004, 144 p.
102. **Siiri Rootsi**. Human Y-chromosomal variation in European populations. Tartu, 2004, 142 p.
103. **Eve Vedler**. Structure of the 2,4-dichloro-phenoxyacetic acid-degradative plasmid pEST4011. Tartu, 2005. 106 p.

104. **Andres Tover**. Regulation of transcription of the phenol degradation *pheBA* operon in *Pseudomonas putida*. Tartu, 2005, 126 p.
105. **Helen Udras**. Hexose kinases and glucose transport in the yeast *Hansenula polymorpha*. Tartu, 2005, 100 p.
106. **Ave Suija**. Lichens and lichenicolous fungi in Estonia: diversity, distribution patterns, taxonomy. Tartu, 2005, 162 p.
107. **Piret Lõhmus**. Forest lichens and their substrata in Estonia. Tartu, 2005, 162 p.
108. **Inga Lips**. Abiotic factors controlling the cyanobacterial bloom occurrence in the Gulf of Finland. Tartu, 2005, 156 p.
109. **Kaasik, Krista**. Circadian clock genes in mammalian clockwork, metabolism and behaviour. Tartu, 2005, 121 p.
110. **Juhan Javoiš**. The effects of experience on host acceptance in ovipositing moths. Tartu, 2005, 112 p.
111. **Tiina Sedman**. Characterization of the yeast *Saccharomyces cerevisiae* mitochondrial DNA helicase Hmi1. Tartu, 2005, 103 p.
112. **Ruth Aguraiuja**. Hawaiian endemic fern lineage *Diellia* (Aspleniaceae): distribution, population structure and ecology. Tartu, 2005, 112 p.
113. **Riho Teras**. Regulation of transcription from the fusion promoters generated by transposition of Tn*4652* into the upstream region of *pheBA* operon in *Pseudomonas putida*. Tartu, 2005, 106 p.
114. **Mait Metspalu**. Through the course of prehistory in india: tracing the mtDNA trail. Tartu, 2005, 138 p.
115. **Elin Lõhmussaar**. The comparative patterns of linkage disequilibrium in European populations and its implication for genetic association studies. Tartu, 2006, 124 p.
116. **Priit Kupper**. Hydraulic and environmental limitations to leaf water relations in trees with respect to canopy position. Tartu, 2006, 126 p.
117. **Heili Ilves**. Stress-induced transposition of Tn*4652* in *Pseudomonas Putida.* Tartu, 2006, 120 p.
118. **Silja Kuusk**. Biochemical properties of Hmi1p, a DNA helicase from *Saccharomyces cerevisiae* mitochondria. Tartu, 2006, 126 p.
119. **Kersti Püssa**. Forest edges on medium resolution landsat thematic mapper satellite images. Tartu, 2006, 90 p.
120. **Lea Tummeleht**. Physiological condition and immune function in great tits (*Parus major* l.): Sources of variation and trade-offs in relation to growth. Tartu, 2006, 94 p.
121. **Toomas Esperk**. Larval instar as a key element of insect growth schedules. Tartu, 2006, 186 p.
122. **Harri Valdmann**. Lynx (*Lynx lynx*) and wolf (*Canis lupus*) in the Baltic region: Diets, helminth parasites and genetic variation. Tartu, 2006. 102 p.
123. **Priit Jõers**. Studies of the mitochondrial helicase Hmi1p in *Candida albicans* and *Saccharomyces cerevisia*. Tartu, 2006. 113 p.
124. **Kersti Lilleväli**. Gata3 and Gata2 in inner ear development. Tartu, 2007, 123 p.

125. **Kai Rünk**. Comparative ecology of three fern species: *Dryopteris carthusiana* (Vill.) H.P. Fuchs, *D. expansa* (C. Presl) Fraser-Jenkins & Jermy and *D. dilatata* (Hoffm.) A. Gray (Dryopteridaceae). Tartu, 2007, 143 p.
126. **Aveliina Helm**. Formation and persistence of dry grassland diversity: role of human history and landscape structure. Tartu, 2007, 89 p.
127. **Leho Tedersoo**. Ectomycorrhizal fungi: diversity and community structure in Estonia, Seychelles and Australia. Tartu, 2007, 233 p.
128. **Marko Mägi**. The habitat-related variation of reproductive performance of great tits in a deciduous-coniferous forest mosaic: looking for causes and consequences. Tartu, 2007, 135 p.
129. **Valeria Lulla**. Replication strategies and applications of Semliki Forest virus. Tartu, 2007, 109 p.
130. **Ülle Reier**. Estonian threatened vascular plant species: causes of rarity and conservation. Tartu, 2007, 79 p.
131. **Inga Jüriado**. Diversity of lichen species in Estonia: influence of regional and local factors. Tartu, 2007, 171 p.
132. **Tatjana Krama**. Mobbing behaviour in birds: costs and reciprocity based cooperation. Tartu, 2007, 112 p.
133. **Signe Saumaa**. The role of DNA mismatch repair and oxidative DNA damage defense systems in avoidance of stationary phase mutations in *Pseudomonas putida.* Tartu, 2007, 172 p.
134. **Reedik Mägi**. The linkage disequilibrium and the selection of genetic markers for association studies in european populations. Tartu, 2007, 96 p.
135. **Priit Kilgas**. Blood parameters as indicators of physiological condition and skeletal development in great tits (*Parus major*): natural variation and application in the reproductive ecology of birds. Tartu, 2007, 129 p.
136. **Anu Albert**. The role of water salinity in structuring eastern Baltic coastal fish communities. Tartu, 2007, 95 p.
137. **Kärt Padari**. Protein transduction mechanisms of transportans. Tartu, 2008, 128 p.
138. **Siiri-Lii Sandre**. Selective forces on larval colouration in a moth. Tartu, 2008, 125 p.
139. **Ülle Jõgar**. Conservation and restoration of semi-natural floodplain meadows and their rare plant species. Tartu, 2008, 99 p.
140. **Lauri Laanisto**. Macroecological approach in vegetation science: generality of ecological relationships at the global scale. Tartu, 2008, 133 p.
141. **Reidar Andreson**. Methods and software for predicting PCR failure rate in large genomes. Tartu, 2008, 105 p.
142. **Birgot Paavel**. Bio-optical properties of turbid lakes. Tartu, 2008, 175 p.
143. **Kaire Torn**. Distribution and ecology of charophytes in the Baltic Sea. Tartu, 2008, 98 p.
144. **Vladimir Vimberg**. Peptide mediated macrolide resistance. Tartu, 2008, 190 p.
145. **Daima Örd**. Studies on the stress-inducible pseudokinase TRB3, a novel inhibitor of transcription factor ATF4. Tartu, 2008, 108 p.

146. **Lauri Saag**. Taxonomic and ecologic problems in the genus *Lepraria* (*Stereocaulaceae*, lichenised *Ascomycota*). Tartu, 2008, 175 p.
147. **Ulvi Karu**. Antioxidant protection, carotenoids and coccidians in greenfinches – assessment of the costs of immune activation and mechanisms of parasite resistance in a passerine with carotenoid-based ornaments. Tartu, 2008, 124 p.
148. **Jaanus Remm**. Tree-cavities in forests: density, characteristics and occupancy by animals. Tartu, 2008, 128 p.
149. **Epp Moks**. Tapeworm parasites *Echinococcus multilocularis* and *E. granulosus* in Estonia: phylogenetic relationships and occurrence in wild carnivores and ungulates. Tartu, 2008, 82 p.
150. **Eve Eensalu**. Acclimation of stomatal structure and function in tree canopy: effect of light and CO_2 concentration. Tartu, 2008, 108 p.
151. **Janne Pullat**. Design, functionlization and application of an *in situ* synthesized oligonucleotide microarray. Tartu, 2008, 108 p.
152. **Marta Putrinš**. Responses of *Pseudomonas putida* to phenol-induced metabolic and stress signals. Tartu, 2008, 142 p.
153. **Marina Semtšenko**. Plant root behaviour: responses to neighbours and physical obstructions. Tartu, 2008, 106 p.
154. **Marge Starast**. Influence of cultivation techniques on productivity and fruit quality of some *Vaccinium* and *Rubus* taxa. Tartu, 2008, 154 p.
155. **Age Tats**. Sequence motifs influencing the efficiency of translation. Tartu, 2009, 104 p.
156. **Radi Tegova**. The role of specialized DNA polymerases in mutagenesis in *Pseudomonas putida.* Tartu, 2009, 124 p.
157. **Tsipe Aavik**. Plant species richness, composition and functional trait pattern in agricultural landscapes – the role of land use intensity and landscape structure. Tartu, 2009, 112 p.
158. **Kaja Kiiver**. Semliki forest virus based vectors and cell lines for studying the replication and interactions of alphaviruses and hepaciviruses. Tartu, 2009, 104 p.
159. **Meelis Kadaja**. Papillomavirus Replication Machinery Induces Genomic Instability in its Host Cell. Tartu, 2009, 126 p.
160. **Pille Hallast**. Human and chimpanzee Luteinizing hormone/Chorionic Gonadotropin beta (*LHB/CGB*) gene clusters: diversity and divergence of young duplicated genes. Tartu, 2009, 168 p.
161. **Ain Vellak**. Spatial and temporal aspects of plant species conservation. Tartu, 2009, 86 p.
162. **Triinu Remmel**. Body size evolution in insects with different colouration strategies: the role of predation risk. Tartu, 2009, 168 p.
163. **Jaana Salujõe**. Zooplankton as the indicator of ecological quality and fish predation in lake ecosystems. Tartu, 2009, 129 p.
164. **Ele Vahtmäe**. Mapping benthic habitat with remote sensing in optically complex coastal environments. Tartu, 2009, 109 p.

165. **Liisa Metsamaa**. Model-based assessment to improve the use of remote sensing in recognition and quantitative mapping of cyanobacteria. Tartu, 2009, 114 p.
166. **Pille Säälik**. The role of endocytosis in the protein transduction by cell-penetrating peptides. Tartu, 2009, 155 p.
167. **Lauri Peil**. Ribosome assembly factors in *Escherichia coli.* Tartu, 2009, 147 p.
168. **Lea Hallik**. Generality and specificity in light harvesting, carbon gain capacity and shade tolerance among plant functional groups. Tartu, 2009, 99 p.
169. **Mariliis Tark**. Mutagenic potential of DNA damage repair and tolerance mechanisms under starvation stress. Tartu, 2009, 191 p.
170. **Riinu Rannap**. Impacts of habitat loss and restoration on amphibian populations. Tartu, 2009, 117 p.
171. **Maarja Adojaan**. Molecular variation of HIV-1 and the use of this knowledge in vaccine development. Tartu, 2009, 95 p.
172. **Signe Altmäe**. Genomics and transcriptomics of human induced ovarian folliculogenesis. Tartu, 2010, 179 p.
173. **Triin Suvi**. Mycorrhizal fungi of native and introduced trees in the Seychelles Islands. Tartu, 2010, 107 p.
174. **Velda Lauringson**. Role of suspension feeding in a brackish-water coastal sea. Tartu, 2010, 123 p.
175. **Eero Talts**. Photosynthetic cyclic electron transport – measurement and variably proton-coupled mechanism. Tartu, 2010, 121 p.
176. **Mari Nelis**. Genetic structure of the Estonian population and genetic distance from other populations of European descent. Tartu, 2010, 97 p.
177. **Kaarel Krjutškov**. Arrayed Primer Extension-2 as a multiplex PCR-based method for nucleic acid variation analysis: method and applications. Tartu, 2010, 129 p.
178. **Egle Köster**. Morphological and genetical variation within species complexes: *Anthyllis vulneraria* s. l. and *Alchemilla vulgaris* (coll.). Tartu, 2010, 101 p.
179. **Erki Õunap**. Systematic studies on the subfamily Sterrhinae (Lepidoptera: Geometridae). Tartu, 2010, 111 p.
180. **Merike Jõesaar**. Diversity of key catabolic genes at degradation of phenol and *p*-cresol in pseudomonads. Tartu, 2010, 125 p.
181. **Kristjan Herkül**. Effects of physical disturbance and habitat-modifying species on sediment properties and benthic communities in the northern Baltic Sea. Tartu, 2010, 123 p.
182. **Arto Pulk**. Studies on bacterial ribosomes by chemical modification approaches. Tartu, 2010, 161 p.
183. **Maria Põllupüü**. Ecological relations of cladocerans in a brackish-water ecosystem. Tartu, 2010, 126 p.
184. **Toomas Silla**. Study of the segregation mechanism of the Bovine Papillomavirus Type 1. Tartu, 2010, 188 p.

185. **Gyaneshwer Chaubey**. The demographic history of India: A perspective based on genetic evidence. Tartu, 2010, 184 p.
186. **Katrin Kepp**. Genes involved in cardiovascular traits: detection of genetic variation in Estonian and Czech populations. Tartu, 2010, 164 p.
187. **Virve Sõber**. The role of biotic interactions in plant reproductive performance. Tartu, 2010, 92 p.
188. **Kersti Kangro**. The response of phytoplankton community to the changes in nutrient loading. Tartu, 2010, 144 p.
189. **Joachim M. Gerhold**. Replication and Recombination of mitochondrial DNA in Yeast. Tartu, 2010, 120 p.
190. **Helen Tammert**. Ecological role of physiological and phylogenetic diversity in aquatic bacterial communities. Tartu, 2010, 140 p.
191. **Elle Rajandu**. Factors determining plant and lichen species diversity and composition in Estonian *Calamagrostis* and *Hepatica* site type forests. Tartu, 2010, 123 p.
192. **Paula Ann Kivistik**. ColR-ColS signalling system and transposition of Tn*4652* in the adaptation of *Pseudomonas putida.* Tartu, 2010, 118 p.
193. **Siim Sõber**. Blood pressure genetics: from candidate genes to genome-wide association studies. Tartu, 2011, 120 p.
194. **Kalle Kipper**. Studies on the role of helix 69 of 23S rRNA in the factor-dependent stages of translation initiation, elongation, and termination. Tartu, 2011, 178 p.
195. **Triinu Siibak**. Effect of antibiotics on ribosome assembly is indirect. Tartu, 2011, 134 p.
196. **Tambet Tõnissoo**. Identification and molecular analysis of the role of guanine nucleotide exchange factor RIC-8 in mouse development and neural function. Tartu, 2011, 110 p.
197. **Helin Räägel**. Multiple faces of cell-penetrating peptides – their intracellular trafficking, stability and endosomal escape during protein transduction. Tartu, 2011, 161 p.
198. **Andres Jaanus**. Phytoplankton in Estonian coastal waters – variability, trends and response to environmental pressures. Tartu, 2011, 157 p.
199. **Tiit Nikopensius**. Genetic predisposition to nonsyndromic orofacial clefts. Tartu, 2011, 152 p.
200. **Signe Värv**. Studies on the mechanisms of RNA polymerase II-dependent transcription elongation. Tartu, 2011, 108 p.
201. **Kristjan Välk**. Gene expression profiling and genome-wide association studies of non-small cell lung cancer. Tartu, 2011, 98 p.
202. **Arno Põllumäe**. Spatio-temporal patterns of native and invasive zooplankton species under changing climate and eutrophication conditions. Tartu, 2011, 153 p.
203. **Egle Tammeleht**. Brown bear (*Ursus arctos*) population structure, demographic processes and variations in diet in northern Eurasia. Tartu, 2011, 143 p.

205. **Teele Jairus**. Species composition and host preference among ectomycorrhizal fungi in Australian and African ecosystems. Tartu, 2011, 106 p.
206. **Kessy Abarenkov**. PlutoF – cloud database and computing services supporting biological research. Tartu, 2011, 125 p.
207. **Marina Grigorova**. Fine-scale genetic variation of follicle-stimulating hormone beta-subunit coding gene (*FSHB*) and its association with reproductive health. Tartu, 2011, 184 p.
208. **Anu Tiitsaar**. The effects of predation risk and habitat history on butterfly communities. Tartu, 2011, 97 p.
209. **Elin Sild**. Oxidative defences in immunoecological context: validation and application of assays for nitric oxide production and oxidative burst in a wild passerine. Tartu, 2011, 105 p.
210. **Irja Saar**. The taxonomy and phylogeny of the genera *Cystoderma* and *Cystodermella* (Agaricales, Fungi). Tartu, 2012, 167 p.
211. **Pauli Saag**. Natural variation in plumage bacterial assemblages in two wild breeding passerines. Tartu, 2012, 113 p.
212. **Aleksei Lulla**. Alphaviral nonstructural protease and its polyprotein substrate: arrangements for the perfect marriage. Tartu, 2012, 143 p.
213. **Mari Järve**. Different genetic perspectives on human history in Europe and the Caucasus: the stories told by uniparental and autosomal markers. Tartu, 2012, 119 p.
214. **Ott Scheler**. The application of tmRNA as a marker molecule in bacterial diagnostics using microarray and biosensor technology. Tartu, 2012, 93 p.
215. **Anna Balikova**. Studies on the functions of tumor-associated mucin-like leukosialin (CD43) in human cancer cells. Tartu, 2012, 129 p.
216. **Triinu Kõressaar**. Improvement of PCR primer design for detection of prokaryotic species. Tartu, 2012, 83 p.
217. **Tuul Sepp**. Hematological health state indices of greenfinches: sources of individual variation and responses to immune system manipulation. Tartu, 2012, 117 p.
218. **Rya Ero**. Modifier view of the bacterial ribosome. Tartu, 2012, 146 p.
219. **Mohammad Bahram**. Biogeography of ectomycorrhizal fungi across different spatial scales. Tartu, 2012, 165 p.
220. **Annely Lorents**. Overcoming the plasma membrane barrier: uptake of amphipathic cell-penetrating peptides induces influx of calcium ions and downstream responses. Tartu, 2012, 113 p.
221. **Katrin Männik**. Exploring the genomics of cognitive impairment: whole-genome SNP genotyping experience in Estonian patients and general population. Tartu, 2012, 171 p.
222. **Marko Prous**. Taxonomy and phylogeny of the sawfly genus *Empria* (Hymenoptera, Tenthredinidae). Tartu, 2012, 192 p.
223. **Triinu Visnapuu**. Levansucrases encoded in the genome of *Pseudomonas syringae* pv. tomato DC3000: heterologous expression, biochemical characterization, mutational analysis and spectrum of polymerization products. Tartu, 2012, 160 p.

224. **Nele Tamberg**. Studies on Semliki Forest virus replication and pathogenesis. Tartu, 2012, 109 p.
225. **Tõnu Esko**. Novel applications of SNP array data in the analysis of the genetic structure of Europeans and in genetic association studies. Tartu, 2012, 149 p.
226. **Timo Arula**. Ecology of early life-history stages of herring *Clupea harengus membras* in the northeastern Baltic Sea. Tartu, 2012, 143 p.
227. **Inga Hiiesalu**. Belowground plant diversity and coexistence patterns in grassland ecosystems. Tartu, 2012, 130 p.
228. **Kadri Koorem**. The influence of abiotic and biotic factors on small-scale plant community patterns and regeneration in boreonemoral forest. Tartu, 2012, 114 p.
229. **Liis Andresen**. Regulation of virulence in plant-pathogenic pectobacteria. Tartu, 2012, 122 p.
230. **Kaupo Kohv**. The direct and indirect effects of management on boreal forest structure and field layer vegetation. Tartu, 2012, 124 p.
231. **Mart Jüssi**. Living on an edge: landlocked seals in changing climate. Tartu, 2012, 114 p.
232. **Riina Klais**. Phytoplankton trends in the Baltic Sea. Tartu, 2012, 136 p.
233. **Rauno Veeroja**. Effects of winter weather, population density and timing of reproduction on life-history traits and population dynamics of moose (*Alces alces*) in Estonia. Tartu, 2012, 92 p.
234. **Marju Keis**. Brown bear (*Ursus arctos*) phylogeography in northern Eurasia. Tartu, 2013, 142 p.
235. **Sergei Põlme**. Biogeography and ecology of *alnus*- associated ectomycorrhizal fungi – from regional to global scale. Tartu, 2013, 90 p.
236. **Liis Uusküla**. Placental gene expression in normal and complicated pregnancy. Tartu, 2013, 173 p.
237. **Marko Lõoke**. Studies on DNA replication initiation in *Saccharomyces cerevisiae.* Tartu, 2013, 112 p.
238. **Anne Aan**. Light- and nitrogen-use and biomass allocation along productivity gradients in multilayer plant communities. Tartu, 2013, 127 p.
239. **Heidi Tamm**. Comprehending phylogenetic diversity – case studies in three groups of ascomycetes. Tartu, 2013, 136 p.
240. **Liina Kangur**. High-Pressure Spectroscopy Study of Chromophore-Binding Hydrogen Bonds in Light-Harvesting Complexes of Photosynthetic Bacteria. Tartu, 2013, 150 p.
241. **Margus Leppik**. Substrate specificity of the multisite specific pseudouridine synthase RluD. Tartu, 2013, 111 p.
242. **Lauris Kaplinski**. The application of oligonucleotide hybridization model for PCR and microarray optimization. Tartu, 2013, 103 p.
243. **Merli Pärnoja**. Patterns of macrophyte distribution and productivity in coastal ecosystems: effect of abiotic and biotic forcing. Tartu, 2013, 155 p.
244. **Tõnu Margus**. Distribution and phylogeny of the bacterial translational GTPases and the Mqsr/YgiT regulatory system. Tartu, 2013, 126 p.

245. **Pille Mänd**. Light use capacity and carbon and nitrogen budget of plants: remote assessment and physiological determinants. Tartu, 2013, 128 p.
246. **Mario Plaas**. Animal model of Wolfram Syndrome in mice: behavioural, biochemical and psychopharmacological characterization. Tartu, 2013, 144 p.
247. **Georgi Hudjašov**. Maps of mitochondrial DNA, Y-chromosome and tyrosinase variation in Eurasian and Oceanian populations. Tartu, 2013, 115 p.
248. **Mari Lepik**. Plasticity to light in herbaceous plants and its importance for community structure and diversity. Tartu, 2013, 102 p.
249. **Ede Leppik**. Diversity of lichens in semi-natural habitats of Estonia. Tartu, 2013, 151 p.
250. **Ülle Saks**. Arbuscular mycorrhizal fungal diversity patterns in boreo-nemoral forest ecosystems. Tartu, 2013, 151 p.
251. **Eneli Oitmaa**. Development of arrayed primer extension microarray assays for molecular diagnostic applications. Tartu, 2013, 147 p.
252. **Jekaterina Jutkina**. The horizontal gene pool for aromatics degradation: bacterial catabolic plasmids of the Baltic Sea aquatic system. Tartu, 2013, 121 p.
253. **Helen Vellau**. Reaction norms for size and age at maturity in insects: rules and exceptions. Tartu, 2014, 132 p.
254. **Randel Kreitsberg**. Using biomarkers in assessment of environmental contamination in fish – new perspectives. Tartu, 2014, 107 p.
255. **Krista Takkis**. Changes in plant species richness and population performance in response to habitat loss and fragmentation.Tartu, 2014, 141 p.
256. **Liina Nagirnaja**. Global and fine-scale genetic determinants of recurrent pregnancy loss. Tartu, 2014, 211 p.
257. **Triin Triisberg**. Factors influencing the re-vegetation of abandoned extracted peatlands in Estonia. Tartu, 2014, 133 p.
258. **Villu Soon**. A phylogenetic revision of the *Chrysis ignita* species group (Hymenoptera: Chrysididae) with emphasis on the northern European fauna. Tartu, 2014, 211 p.
259. **Andrei Nikonov**. RNA-Dependent RNA Polymerase Activity as a Basis for the Detection of Positive-Strand RNA Viruses by Vertebrate Host Cells. Tartu, 2014, 207 p.
260. **Eele Õunapuu-Pikas**. Spatio-temporal variability of leaf hydraulic conductance in woody plants: ecophysiological consequences. Tartu, 2014, 135 p.
261. **Marju Männiste**. Physiological ecology of greenfinches: information content of feathers in relation to immune function and behavior. Tartu, 2014, 121 p.
262. **Katre Kets**. Effects of elevated concentrations of CO_2 and O_3 on leaf photosynthetic parameters in *Populus tremuloides*: diurnal, seasonal and interannual patterns. Tartu, 2014, 115 p.

263. **Külli Lokko**. Seasonal and spatial variability of zoopsammon communities in relation to environmental parameters. Tartu, 2014, 129 p.
264. **Olga Žilina**. Chromosomal microarray analysis as diagnostic tool: Estonian experience. Tartu, 2014, 152 p.
265. **Kertu Lõhmus**. Colonisation ecology of forest-dwelling vascular plants and the conservation value of rural manor parks. Tartu, 2014, 111 p.
266. **Anu Aun**. Mitochondria as integral modulators of cellular signaling. Tartu, 2014, 167 p.
267. **Chandana Basu Mallick**. Genetics of adaptive traits and gender-specific demographic processes in South Asian populations. Tartu, 2014, 160 p.
268. **Riin Tamme**. The relationship between small-scale environmental heterogeneity and plant species diversity. Tartu, 2014, 130 p.
269. **Liina Remm**. Impacts of forest drainage on biodiversity and habitat quality: implications for sustainable management and conservation. Tartu, 2015, 126 p.
270. **Tiina Talve**. Genetic diversity and taxonomy within the genus *Rhinanthus.* Tartu, 2015, 106 p.
271. **Mehis Rohtla**. Otolith sclerochronological studies on migrations, spawning habitat preferences and age of freshwater fishes inhabiting the Baltic Sea. Tartu, 2015, 137 p.
272. **Alexey Reshchikov**. The world fauna of the genus *Lathrolestes* (Hymenoptera, Ichneumonidae). Tartu, 2015, 247 p.
273. **Martin Pook**. Studies on artificial and extracellular matrix protein-rich surfaces as regulators of cell growth and differentiation. Tartu, 2015, 142 p.
274. **Mai Kukumägi**. Factors affecting soil respiration and its components in silver birch and Norway spruce stands. Tartu, 2015, 155 p.
275. **Helen Karu**. Development of ecosystems under human activity in the North-East Estonian industrial region: forests on post-mining sites and bogs. Tartu, 2015, 152 p.
276. **Hedi Peterson**. Exploiting high-throughput data for establishing relationships between genes. Tartu, 2015, 186 p.
277. **Priit Adler**. Analysis and visualisation of large scale microarray data, Tartu, 2015, 126 p.
278. **Aigar Niglas**. Effects of environmental factors on gas exchange in deciduous trees: focus on photosynthetic water-use efficiency. Tartu, 2015, 152 p.
279. **Silja Laht**. Classification and identification of conopeptides using profile hidden Markov models and position-specific scoring matrices. Tartu, 2015, 100 p.
280. **Martin Kesler**. Biological characteristics and restoration of Atlantic salmon *Salmo salar* populations in the Rivers of Northern Estonia. Tartu, 2015, 97 p.
281. **Pratyush Kumar Das**. Biochemical perspective on alphaviral nonstructural protein 2: a tale from multiple domains to enzymatic profiling. Tartu, 2015, 205 p

282. **Priit Palta**. Computational methods for DNA copy number detection. Tartu, 2015, 130 p.
283. **Julia Sidorenko**. Combating DNA damage and maintenance of genome integrity in pseudomonads. Tartu, 2015, 174 p.
284. **Anastasiia Kovtun-Kante**. Charophytes of Estonian inland and coastal waters: distribution and environmental preferences. Tartu, 2015, 97 p.
285. **Ly Lindman**. The ecology of protected butterfly species in Estonia. Tartu, 2015, 171 p.
286. **Jaanis Lodjak**. Association of Insulin-like Growth Factor I and Corticosterone with Nestling Growth and Fledging Success in Wild Passerines. Tartu, 2016, 113 p.
287. **Ann Kraut**. Conservation of Wood-Inhabiting Biodiversity – Semi-Natural Forests as an Opportunity. Tartu, 2016, 141 p.
288. **Tiit Örd.** Functions and regulation of the mammalian pseudokinase TRIB3. Tartu, 2016, 182. p.
289. **Kairi Käiro.** Biological Quality According to Macroinvertebrates in Streams of Estonia (Baltic Ecoregion of Europe): Effects of Human-induced Hydromorphological Changes. Tartu, 2016, 126 p.
290. **Leidi Laurimaa**. *Echinococcus multilocularis* and other zoonotic parasites in Estonian canids. Tartu, 2016, 144 p.
291. **Helerin Margus.** Characterization of cell-penetrating peptide/nucleic acid nanocomplexes and their cell-entry mechanisms. Tartu, 2016, 173 p.
292. **Kadri Runnel**. Fungal targets and tools for forest conservation. Tartu, 2016, 157 p.
293. **Urmo Võsa**. MicroRNAs in disease and health: aberrant regulation in lung cancer and association with genomic variation. Tartu, 2016, 163 p.
294. **Kristina Mäemets-Allas**. Studies on cell growth promoting AKT signaling pathway – a promising anti-cancer drug target. Tartu, 2016, 146 p.
295. **Janeli Viil.** Studies on cellular and molecular mechanisms that drive normal and regenerative processes in the liver and pathological processes in Dupuytren's contracture. Tartu, 2016, 175 p.
296. **Ene Kook**. Genetic diversity and evolution of *Pulmonaria angustifolia* L. and *Myosotis laxa sensu lato* (Boraginaceae). Tartu, 2016, 106 p.
297. **Kadri Peil.** RNA polymerase II-dependent transcription elongation in *Saccharomyces cerevisiae*. Tartu, 2016, 113 p.
298. **Katrin Ruisu.** The role of RIC8A in mouse development and its function in cell-matrix adhesion and actin cytoskeletal organisation. Tartu, 2016, 129 p.
299. **Janely Pae**. Translocation of cell-penetrating peptides across biological membranes and interactions with plasma membrane constituents. Tartu, 2016, 126 p.
300. **Argo Ronk.** Plant diversity patterns across Europe: observed and dark diversity. Tartu, 2016, 153 p.

301. **Kristiina Mark**. Diversification and species delimitation of lichenized fungi in selected groups of the family Parmeliaceae (Ascomycota). Tartu, 2016, 181 p.
302. **Jaak-Albert Metsoja**. Vegetation dynamics in floodplain meadows: influence of mowing and sediment application. Tartu, 2016, 140 p.
303. **Hedvig Tamman.** The GraTA toxin-antitoxin system of *Pseudomonas putida*: regulation and role in stress tolerance. Tartu, 2016, 154 p.
304. **Kadri Pärtel**. Application of ultrastructural and molecular data in the taxonomy of helotialean fungi. Tartu, 2016, 183 p.
305. **Maris Hindrikson**. Grey wolf (*Canis lupus*) populations in Estonia and Europe: genetic diversity, population structure and -processes, and hybridization between wolves and dogs. Tartu, 2016, 121 p.
306. **Polina Degtjarenko**. Impacts of alkaline dust pollution on biodiversity of plants and lichens: from communities to genetic diversity. Tartu, 2016, 126 p.
307. **Liina Pajusalu**. The effect of CO_2 enrichment on net photosynthesis of macrophytes in a brackish water environment. Tartu, 2016, 126 p.
308. **Stoyan Tankov**. Random walks in the stringent response. Tartu, 2016, 94 p.
309. **Liis Leitsalu**. Communicating genomic research results to population-based biobank participants. Tartu, 2016, 158 p.
310. **Richard Meitern**. Redox physiology of wild birds: validation and application of techniques for detecting oxidative stress. Tartu, 2016, 134 p.
311. **Kaie Lokk**. Comparative genome-wide DNA methylation studies of healthy human tissues and non-small cell lung cancer tissue. Tartu, 2016, 127 p.
312. **Mihhail Kurašin.** Processivity of cellulases and chitinases. Tartu, 2017, 132 p.
313. **Carmen Tali.** Scavenger receptors as a target for nucleic acid delivery with peptide vectors. Tartu, 2017, 155 p.
314. **Katarina Oganjan**. Distribution, feeding and habitat of benthic suspension feeders in a shallow coastal sea. Tartu, 2017, 132 p.
315. **Taavi Paal.** Immigration limitation of forest plants into wooded landscape corridors. Tartu, 2017, 145 p.
316. **Kadri Õunap**. The Williams-Beuren syndrome chromosome region protein WBSCR22 is a ribosome biogenesis factor. Tartu, 2017, 135 p.
317. **Riin Tamm**. In-depth analysis of factors affecting variability in thiopurine methyltransferase activity. Tartu, 2017, 170 p.
318. **Keiu Kask**. The role of RIC8A in the development and regulation of mouse nervous system. Tartu, 2017, 184 p.
319. **Tiia Möller**. Mapping and modelling of the spatial distribution of benthic macrovegetation in the NE Baltic Sea with a special focus on the eelgrass *Zostera marina* Linnaeus, 1753. Tartu, 2017, 162 p.
320. **Silva Kasela**. Genetic regulation of gene expression: detection of tissue- and cell type-specific effects. Tartu, 2017, 150 p.

321. **Karmen Süld.** Food habits, parasites and space use of the raccoon dog *Nyctereutes procyonoides*: the role of an alien species as a predator and vector of zoonotic diseases in Estonia. Tartu, 2017, p.
322. **Ragne Oja.** Consequences of supplementary feeding of wild boar – concern for ground-nesting birds and endoparasite infection. Tartu, 2017, 141 p.